An Engineering Assessment of Acoustic Methods of Leak Detection in Aboveground Storage Tanks

HEALTH AND ENVIRONMENTAL AFFAIRS
API PUBLICATION NUMBER 307
JANUARY 1992

American Petroleum Institute
1220 L Street, Northwest
Washington, D.C. 20005

An Engineering Assessment of Acoustic Methods of Leak Detection in Aboveground Storage Tanks

Health and Environmental Affairs Department
API PUBLICATION NUMBER 307
JANUARY 1992

PREPARED UNDER CONTRACT BY:
ERIC G. ECKERT AND JOSEPH W. MARESCA, JR.
VISTA RESEARCH, INC.
MOUNTAIN VIEW, CA

American Petroleum Institute

FOREWORD

API PUBLICATIONS NECESSARILY ADDRESS PROBLEMS OF A GENERAL NATURE. WITH RESPECT TO PARTICULAR CIRCUMSTANCES, LOCAL, STATE, AND FEDERAL LAWS AND REGULATIONS SHOULD REVIEWED.

API IS NOT UNDERTAKING TO MEET THE DUTIES OF EMPLOYERS, MANUFACTURERS, OR SUPPLIERS TO WARN AND PROPERLY TRAIN AND EQUIP THEIR EMPLOYEES, AND OTHERS EXPOSED, CONCERNING HEALTH AND SAFETY RISKS AND PRECAUTIONS, NOR UNDERTAKING THEIR OBLIGATIONS UNDER LOCAL, STATE, OR FEDERAL LAWS.

NOTHING CONTAINED IN ANY API PUBLICATION IS TO BE CONSTRUED AS GRANTING ANY RIGHT, BY IMPLICATION OR OTHERWISE, FOR THE MANUFACTURE, SALE, OR USE OF ANY METHOD, APPARATUS, OR PRODUCT COVERED BY LETTERS PATENT. NEITHER SHOULD ANYTHING CONTAINED IN THE PUBLICATION BE CONSTRUED AS INSURING ANYONE AGAINST LIABILITY FOR INFRIGEMENT OF LETTERS PATENT.

Table of Contents

Executive Summary

Introduction

Though a number of firms offer aboveground storage tank (AST) leak detection services based on passive acoustics, very little information has been published concerning the performance of such systems or the nature of the acoustic leak signal. This document provides the results of an engineering assessment of passive-acoustic sensing methods for detecting small leaks in large ASTs.[1] The assessment consisted of laboratory experiments, analyses of unpublished data collected by industry in a 10-foot-diameter AST containing water, and field experiments at the Mobil Oil Refinery in Beaumont, Texas on a 114-foot-diameter AST containing a heavy naphtha petroleum product.

Background

The American Petroleum Institute (API) has completed two phases of a leak detection project for aboveground storage tanks (ASTs). The purpose of Phase I was to assess different leak detection technologies to determine which had the greatest potential for field application. Because acoustic and volumetric methods were found to have significant operational and performance advantages, they were the ones chosen for testing under Phase II of the project.

The purpose of Phase II was to perform an engineering assessment of acoustic and volumetric methods for detecting small leaks in large ASTs. The principal objectives of Phase II were:

- to determine, in the case of acoustic methods, the nature of the leak signal and the ambient noise in an AST;
- to determine, in the case of volumetric methods, the sources and magnitude of ambient noise associated with measurements in an AST;
- to perform field experiments on a large, full-scale AST; and
- to recommend ways to improve existing AST leak detection methods.

Conclusions

The analytical and experimental results of this project suggest that a passive-acoustic system can be used to detect small leaks in ASTs. The experiments have shown that a detectable leak signal does exist, but that the current approach to data acquisition and signal processing needs to be improved for the technology to achieve its full potential. As part of the field tests under Phase II, an algorithm based on radar beam-forming techniques was developed; this algorithm improved the detection of leaks. An example of the application of the algorithm to both impulsive and continuous leak signals is presented in this report. Both the beam-forming algorithm and the data collection strategy must be evaluated by means of further experiments designed to estimate the performance of a passive-acoustic system in the presence of real leaks in the floor of an AST. Section 3 of the body of this report consists of a short but detailed summary of the technical results of this engineering assessment. A description of the experimments and analyses are presented in two professional papers, which are attached as appendices to the report.

---

1 The results of the volumetric study are provided in a separate API document entitled *An Engineering Assessment of Volumetric Methods of Leak Detection in Aboveground Storage Tanks*, by James W. Starr and Joseph W. Maresca, Jr.

1 Introduction

This report summarizes Phase II of a research program conducted by the American Petroleum Institute (API) to evaluate the performance of technologies that can be used to detect leaks in the floors of aboveground storage tanks. During Phase I, an analytical assessment of the performance four leak detection technologies was investigated [1, 2]. The four technologies included: (1) passive-acoustic sensing systems, (2) volumetric systems, especially differential pressure (or "mass") measurement systems, (3) advanced inventory reconciliation methods, and (4) tracers methods. During Phase II, field tests were conducted on an aboveground storage tank to make an engineering assessment of the performance of two of these technologies, passive-acoustic sensing systems and volumetric detection systems. This report describes the engineering assessment of the acoustic systems that were examined; the engineering assessment of volumetric systems is described in a separate report [3].

The specific objectives of the Phase II research in the area of acoustics were to:

- assess the current state of AST leak detection technology
- determine the nature of the leak signal and the ambient acoustic noise in an AST
- perform field experiments on a full-scale AST
- recommend ways to improve existing AST detection systems

The field tests were conducted at the Mobil Oil Refinery in Beaumont, Texas, on a 50,000-bbl, 114-ft-diameter AST containing a heavy naphtha petroleum product. The experiments focused on identifying and quantifying the acoustic leak signal and its source mechanisms, and on formulating the strategies necessary to detect the leak signal.

2 Background

The choice of a particular strategy for the collection and processing of acoustic signals is strongly tied to the nature of the signal and the background noise field in which the signal is immersed. The approach to AST acoustic leak detection adopted by the industry is based upon the success with which flaws and cracks in a variety of materials have been identified through the use of acoustic emissions (AE) techniques, and the ease with which such systems may be designed and operated. Though a number of firms offer AST leak detection services based upon passive acoustics, very little technical information has been published concerning the performance of such systems or the nature of the acoustic leak signal. While tank owners and operators covet the operational features of the technology, there is a need to provide convincing evidence that the technology is effective. A first step toward providing this evidence is to review the few available test results provided by the leak detection industry and to perform a system analysis of the data collection and processing approach being used. The assessment of passive acoustic leak detection technology presented in this work is based both on the industry-derived data and on laboratory and field experiments.

The current method by which the presence of an AST leak is inferred is detection-through-location. In order to locate a region of the AST floor that emits acoustic energy in excess of a measured, average level, an array of transducers is used to construct a sound-level map. Currently available acoustic leak detection systems require that the leak emit impulsive signals whose amplitude greatly exceeds the background noise level. The process of converting these impulsive signals into a sound-level map can be described as follows. For each element of the sensor array, an impulse arrival time is recorded when a preset threshold signal level is exceeded. Sets of impulse arrival times then serve as input to a location algorithm that predicts the most likely origin of the signal. A large number of such location predictions are plotted on a diagram of the AST floor to produce the sound-level map. Regions of the map in which significant clustering of source locations is observed are interpreted as likely leak locations. Published results of field tests on full-scale ASTs, and unpublished results made available for review, offer little convincing evidence that this approach to passive-acoustic leak detection performs adequately when applied to the AST leak detection problem. An analysis of the problems associated with the current generation of leak detection systems was performed in which two fundamental questions were addressed. First, are large-amplitude, impulsive signals (i.e., background noise) expected to dominate the acoustic signal in the case of real AST leaks? Secondly, if leak-generated impulsive signals exist, are they being acquired and processed correctly?

3 Summary of Results

The nature of both the acoustic leak signal and its corresponding source mechanisms was investigated in a series of laboratory experiments. A leak simulator was constructed in order to control the flow rate, backfill material, and pressure head above the leak. Time series of acoustic signals were recorded by a pair of transducers placed in close proximity to the leak. The results of these experiments showed that the acoustic leak signal is comprised of both impulsive and continuous components. Turbulent flow, cavitation, and particulates in the backfill colliding with each other and with the tank floor were identified as the most likely source mechanisms for the production of continuous leak signals. The interaction between the leak flow field and air bubbles trapped within the backfill material was the only source mechanism found to produce the large-amplitude, impulsive signals upon which the current leak detection technology is based. In addition, once the backfill material became fully saturated, the production of impulses ceased. These results brought into question the persistence of impulsive leak signals in an operational AST, but also identified detectable, persistent signals that have not yet been exploited by the industry.

The published results of field tests show a high degree of scatter in the data used to form sound-level maps. On the assumption that the backfill conditions present during these tests were appropriate for the production of impulsive leak signals, an analysis was made of the data collection and signal processing methods currently employed by the testing industry. The results of this study indicate that the manner in which data are acquired, i.e., collecting a set of impulse arrival times whenever a threshold exceedance occurs on any element of the sensor array, tends to produce inaccurate location estimates in proportion to the rate at which impulses are emitted from the leak. When only impulse arrival times are collected, as opposed to continuous time series, the possibility exists that a given set of arrival times are not correlated with the emission of a single impulsive signal, but instead are correlated with two or more distinct events. The processing of these mixed-arrival time sets by the location algorithm was suggested as a probable source of error. For a full-scale tank, it was shown that the inaccurate collection of impulsive signals would occur 50% of the time for a rate of impulse emission of only 12 s^{-1}. This analysis assumed that the noise was zero and that only detectable signals were present; the percentage of improperly collected signals would increase significantly if noise were included or the rate of impulse emission were increased.

The detectability of acoustic leak signals and alternative methods for the processing of these signals were investigated through the analysis of data obtained during field tests on 10- and 114-ft-diameter ASTs. One of the vendors provided continuous time series of impulsive leak signals recorded in a 10-ft-diameter AST by internal hydrophones and external resonant sensors. The primary results of this analysis were that: (1) impulsive signals dominated the acoustic leak signal produced in a 10-ft-diameter test tank, and (2) the impulses were detected equally well by external and internal sensors. The presence of impulsive leak signals in the test-tank data is consistent with the laboratory results cited above. The backfill material was well drained, thus allowing for the entrainment of air bubbles into the leak flow field.

An extensive series of tests were conducted on a 114-ft-diameter AST located at the Mobil Oil Refinery in Beaumont, Texas. The primary goals of the Beaumont experiment were to: (1) investigate the detectability of impulsive-vs.-continuous acoustic leak signals, (2) measure the ambient noise field against which the leak signals must be detected, and (3) obtain continuous time series on a variety of sensor arrays so that improved detection algorithms could be tested. In order to gain a degree of control over the presence or absence of the leak signal, and over the source mechanisms that give rise to the leak signal, a pair of leak simulators were constructed for use in the AST. Both impulsive and continuous components of the simulated acoustic leak signal were found to be detectable in an AST of this dimension. The character of the impulsive leak signal produced by leakage into partially saturated backfills was such that currently used data collection and signal processing techniques would be unlikely to detect the leak in a reliable, convincing manner. The ambient noise field was found to be strongest at frequencies below 10 kHz, thus masking a substantial portion of the continuous leak signal received by external sensors. Because the typical AST leak signal will most likely be influenced by a variety of source mechanisms, the possibility that both impulsive and continuous signals can be processed by the *same* detection algorithm was investigated. A leak detection algorithm based upon beam-forming techniques was applied to the impulsive and continuous leak signals collected during the Beaumont test. Good agreement between the predicted and actual leak location was obtained for both types of signals.

The analytical and experimental results of this project are very encouraging, suggesting as they do that a passive-acoustic system would be capable of detecting small leaks in ASTs. These experiments have shown that a detectable leak signal does exist, but that the current approach to data acquisition and signal processing needs to be improved for the technology to achieve its full potential. The beam-forming algorithm developed to detect a broad range of acoustic leak signals may provide a means of detection that is largely independent of the particular source mechanisms associated with a given AST leak. The beam-forming detection algorithm and data acquisition system should be refined by means of experimental data obtained from a sensor array that contains a large number of optimally spaced elements. In addition, the uncertainty concerning the character of the signals produced by real AST leaks must be addressed through further experiments.

4 Report Organization

The work performed as part of the Phase II program is summarized in two technical papers prepared for publication in the engineering and scientific literature. A copy of each paper is presented, respectively, in Appendices A and B of this report. Both papers describe the results of the experiments with the passive-acoustic sensing system. One has already been published [4], and the other [5] will be submitted for publication shortly.

The paper attached as Appendix A [4] provides a description of the current generation of AE-based leak detection systems and presents the results of an analysis of the data collection and signal processing procedures being used by these systems. This paper also presents an analysis of data that were collected on a 10-ft-diameter AST by a vendor and that were subsequently provided to the API. These data were analyzed for the purpose of investigating the nature of impulsive leak-signal propagation and the detection of impulsive signals by internal vs. external sensors. Finally, the paper presents the results of an extensive set of laboratory experiments in which the nature of the leak signal and its source mechanisms was investigated.

The paper attached as Appendix B [5] describes the field experiments conducted on a 114-ft-diameter AST and a test of a detection algorithm based on the principles of classical beam forming. Source mechanisms identified in [4] were produced through the use of a leak simulator placed inside the AST. The detectability of acoustic leak signals over typical AST dimensions was investigated. This was done by recording continuous time series with arrays of sensors mounted on the external wall of the tank and with a pair of hydrophones deployed internally. Suggestions for improved performance of passive-acoustic leak detection systems are based on the results of these field experiments, and on the development of data collection and signal processing techniques appropriate for the detection of a broad class of relatively weak acoustic leak signals against a strong ambient noise field.

References

1. J. W. Starr and J. W. Maresca, Jr. "Leak Detection Technologies for Aboveground Storage Tanks When In Service." Final Report for the American Petroleum Institute, Vista Research Project 2032, Vista Research, Inc., Mountain View, California (August 1989).

2. J. W. Maresca, Jr., and J. W. Starr. "Aboveground Tank Leak Detection Technologies." *Proceedings of the 10th Annual ILTA Operating Conference*, Houston, Texas (June 1990).

3. J. W. Starr and J. W. Maresca, Jr. "An Engineering Assessment of Volumetric Methods of Leak Detection in Aboveground Storage Tanks." Final Report for the American Petroleum Institute, Vista Research, Inc., Mountain View, California (25 October 1991).

4. E. G. Eckert and J. W. Maresca, Jr. "Detection of Leaks in the Floor of Aboveground Storage Tanks by Means of a Passive Acoustic Sensing System." *Proceedings of the 84th Annual Meeting and Exposition of the Air and Waste Management Association,* Vancouver, B.C. (16-21 June 1991).

5. E. G. Eckert and J. W. Maresca, Jr. "Field Tests of Passive Acoustic Leak Detection Systems for Aboveground Storage Tanks When In Service." Final Report, American Petroleum Institute, Vista Research Project 2032, Vista Research, Inc., Mountain View, California (to be submitted for publication).

Appendix A

Detection of Leaks in the Floor of Aboveground Storage Tanks by Means of a Passive Acoustic Sensing System

E. G. Eckert and J. W. Maresca, Jr.

Vista Research, Inc.
Mountain View, California

This paper was published by the Air and Waste Management Association in its *Proceedings of the 24th Annual Meeting and Exhibition* held in Vancouver, British Columbia, on 16-20 June 1991. The paper contained in this appendix is essentially the same as the one published by the Air and Waste Management Association, except that a correction was made to Figure 6, which had inadvertently been reversed in the original.

The description of data collection and processing found in the section of the paper entitled "Description of Commercially Available Acoustic Leak Detection Systems" (and the analysis based on this description in the section entitled "Impulse-Mixing Analysis") is based on the system used by one of the firms that offers acoustic testing services. It should be noted that several firms, upon reviewing the data collection and processing method described in the paper, pointed out that their methods differed slightly from the one described and were actually more complex and robust. While this may be true, it is the opinion of the authors that the conclusions of the impulse-mixing analysis would not change materially even if this analysis were done repeatedly in such a way as to model more precisely the methodology used by *each* of the firms providing services or systems for detection.

Detection of Leaks in the Floor of Aboveground Storage Tanks by Means of a Passive Acoustic Sensing System

Eric G. Eckert and Joseph W. Maresca, Jr.

Vista Research, Inc.
P. O. Box 998
Mountain View, California 94042

Abstract

The acoustic signal produced by a leak in the floor of an aboveground storage tank (AST) was investigated through laboratory and field experiments. Detectable leak signals observed under laboratory conditions were found to be caused by three primary source mechanisms: (1) turbulent flow through the leak aperture, (2) particulate collisions with the tank floor, and (3) air bubble/flowfield interactions. While turbulent flow noise was present in all recorded leak signals, mechanisms (2) and (3) were strongly dependent on backfill conditions. Leak signals recorded in a 10-ft-diameter AST were analyzed in order to verify the existence of the impulsive leak signal, to investigate the propagation mode of leak signals, and to determine the detection/location capability of a narrow-aperture, three-dimensional acoustic array suspended in the fluid. Successful location of a 2-mm hole in the floor of the 10-ft-diameter tank was accomplished by applying a least squares estimation algorithm to the data obtained from the submerged acoustic array. A statistical analysis of the data collection procedures currently being used shows that frequent false alarms and missed detections result from improper time registration of impulsive leak signals. Several recommendations for minimizing this problem are made.

Introduction

Detection of small leaks in the floor of a large aboveground storage tank (AST) is an extremely difficult task. The American Petroleum Institute (API) has undertaken a program to evaluate the performance of different technologies for detecting small leaks. During Phase 1 of the program, the API described and made a preliminary analysis of the operational and performance features of four technologies[1,2]. During Phase 2, it will conduct a set of experiments in a 77,300-barrel (3.3-Mgal), 117-ft-diameter AST in Beaumont, Texas. These experiments will investigate the important sources of noise and signal-plus-noise of two leak detection approaches, one using an array of passive acoustic sensors and another using mass/volumetric measurement systems. This paper provides a description of commercially available acoustic detection systems and a preliminary assessment of the technology for detection of leaks in large tanks.

Passive acoustic detection systems play an important role in successfully identifying structural defects in a wide variety of materials. The use of acoustic systems to detect leaks in the floor of an AST evolved from and is based on the technology used to detect flaws and cracks in the walls of a pressurized vessel by means of acoustic emissions. A distinction should be made between an acoustic emission associated with the concentration of stresses in a material and the hydrodynamic acoustic signal produced by a small leak in an AST floor. While many important AST structural problems can be identified through acoustic emissions, the techniques used to acquire and process acoustic emissions data may not be applicable to detecting the acoustic signal produced by a leak.

A review of the industry shows that firms providing acoustic leak detection services for ASTs have been involved principally in using acoustic emissions techniques. The main differences in the acoustic systems used by each firm are the type of sensors and the type of arrays. In general, all of the firms use the same approach to data collection and analysis. This technology is desirable from an operational standpoint because tests can be conducted with only minimal disruption to transfer operations. The sensors are mounted on the outside wall of the tank and a test can be conducted in a short time (approximately 1 h).

The performance of this technology for detecting leaks in the floor of ASTs is at present unknown. A review of the literature shows that very little technical information is available to evaluate the capability of acoustic technology. Most of the technical information has not been published because it is considered proprietary. Of the papers that have been published, most concentrate primarily on the results of leak detection tests but do not adequately describe the fundamentals of the technology. One paper describes some laboratory and small-tank experiments with water[3], suggesting that a detectable signal exists, but does not describe the character of the signal or how to detect it. Another paper describes the results of some field tests of an acoustic leak detection system[4]. These tests were designed to demonstrate the technology and do not investigate the background noise or the characteristics of the signal, which are required to estimate the performance of a system. Unfortunately, these field tests, which are supposedly a good example of the technology, are not overwhelmingly convincing even as a demonstration. This same statement is true of other unpublished demonstrations conducted by other testing services. As a result of this paucity of technical information and the lack of overwhelmingly convincing leak detection demonstrations, tank owners and operators, while they covet the operational features of the technology, are unable to determine whether this technology is effective.

The performance of a leak detection system depends on how easy or difficult it is to unambiguously identify the signal in the presence of the noise. The noise is any acoustic return produced by either the instrumentation, or any man-made or ambient source that has characteristics similar to the signal. If the signal can be isolated from the noise, then performance will be high; if not, performance will be poor. The objective of the data collection and signal processing is to minimize the noise. In order to do this, the first step is to determine the basic characteristics of the signal. This paper addresses the signal. It does not address the magnitude and frequency content of the potential sources of ambient noise that might be encountered during a leak detection test. Until the ambient noise field is addressed, however, no estimates of performance are possible. The magnitude of the ambient noise field and its frequency content will be identified during Phase 2 of the API program, through field tests in an operational 117-ft-diameter tank containing light petroleum products.

A number of important questions are addressed in this paper.

- What are the current approaches to acoustic leak detection and how effective are they?
- Does a leak signal exist? If it does, what is it, how is it affected by backfill, how does it propagate, and how detectable is it?
- What approaches to data collection, array configuration, and signal processing can be used to enhance performance?

The analysis and experiments reported herein were completed in support of the design of field tests on a 117-ft-diameter tank and are part of a preliminary evaluation of the technology by the API. This paper consists of the analysis of the data from (1) three experiments conducted and provided by DNV Industrial Services, Inc., (2) laboratory experiments conducted by Vista Research, Inc., using sensors and amplifiers provided by Hartford Steam Boiler Inspection Technologies, and (3) published data from MQS Inspection, Inc.[4]. The results of the analyses presented in this paper suggests that the technology has high potential for detection of leaks in the floor of an AST, but performance is hampered by the way in which data is currently being collected and processed.

Description of Commercially Available Acoustic Leak Detection Systems

Acoustic leak detection systems currently available in the United States are designed to detect impulsive signals in the time domain that are much larger than the background noise level. The acoustic signal is sampled by a multi-channel transient recorder at a very high rate (e.g., 1 MHz), and an array of frequency-selective sensors is used to acquire data for a time-of-arrival analysis. (Examples of time series that contain impulsive leak signals are shown in Figures 4 and 14.) It is assumed by leak detection firms that these large impulsive signals exist and that multiple signals can be uniquely distinguished in time from one another. The procedure by which a set of impulse arrival times is acquired from the acoustic array is as follows: a threshold signal level is set and whenever it is exceeded at one sensor, the time of arrival of the next threshold exceedance at each sensor in the array is recorded. This is done during a preset window, after which time no further data are admitted. A second window allows for multipath and reverberation signals to diminish. After the second window has passed, the transient recorder again begins sampling the acoustic signals until another threshold exceedance occurs at one of the sensors. The transient recorders used here can process up to 2000 threshold exceedances per minute. Though the data acquisition systems currently employed by testing firms are able to record time series of the acoustic leak signals as well as impulse arrival times, this capability has not been exploited for the purpose of leak detection. The threshold is set low to ensure that the leak signal is not missed. Discussions with the testing services indicate that the thresholds are set near the peak values of the background noise between the large impulsive signals the systems are designed to detect. As a consequence, many threshold exceedances occur during a test, and it is likely that many of these exceedances are simply the result of large noise fluctuations. (It should be pointed out that the testing services have many restrictions on when a test can be conducted. To minimize the ambient noise fluctuations, for example, tests are not conducted if it is raining or if the wind velocity is too high.) Given a set of impulse arrival times, the location of the impulse source is estimated through the application of a triangulation algorithm. This analysis assumes that each sensor receives a signal from the same impulsive event; false locations will occur if this assumption is violated. These false locations will increase the probabilities of false alarms and missed detections.

Figure 1 illustrates three types of acoustic arrays currently used by the testing services. The first array, shown in Figure 1(a), consists of 12 sensors spaced uniformly around the circumference of the tank. The sensors are located near the bottom of the tank, but above any sludge that might accumulate. In a 100-ft-diameter tank, the 30° spacing results in a 26-ft separation between sensors. The second array, shown in Figure 1(b), is similar to the first, but with the addition of a vertical element. In this array, 6 sensors spaced at 60° intervals are used. The vertical sensor is used to distinguish signals arriving from the top of the tank. For the purposes of discussion in this paper, these types of arrays will be called wide-aperture arrays. In Figure 1(c), a narrow-aperture array is shown. This array consists of 6 sensors positioned along the circumference of a circle that is less than 1 m in diameter. The array is attached directly to the external wall of a tank. To avoid shadowing of the signal, this array is sometimes located at two or more different positions around the circumference of the tank. This circular array has both vertical and horizontal elements. Since the sensors in all three arrays are attached directly to the wall for the measurements, good contact between the sensor and the wall is important.

The data obtained from each threshold exceedance is analyzed in real time and the estimated source locations are then plotted graphically; the number of threshold exceedances (i.e., hits) depends on the number of the sensors in the array and the nature of the analysis. If the source location is outside the circumference of the tank it is identified as a false hit and removed from the analysis. The vertical sensors are used to discriminate against impulses that do not

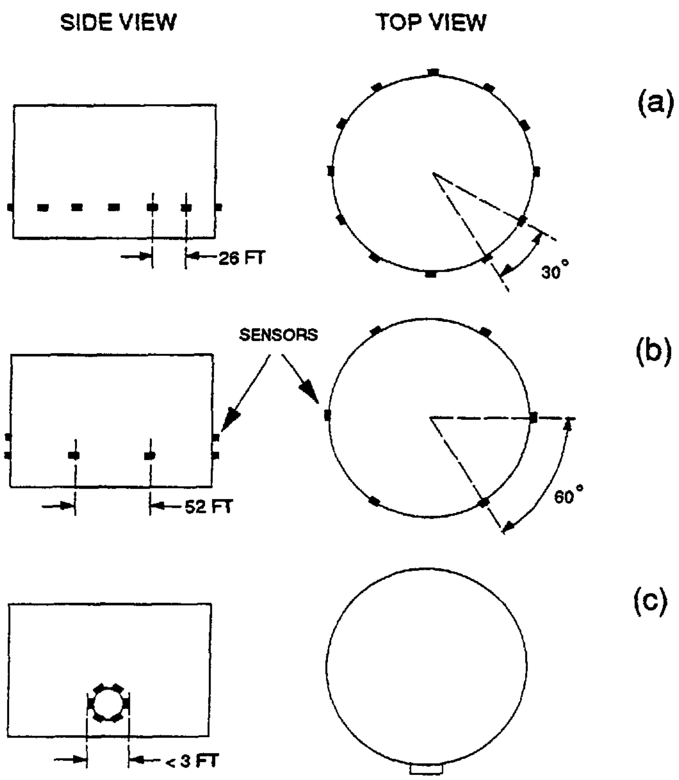

Figure 1. Three sensor array geometries being used by commercial testing services: (a) wide-aperture horizontal array, (b) wide-aperture horizontal array with vertical elements, and (c) narrow-aperture array with horizontal and vertical elements.

arrive from the bottom of the tank. In addition to the measurement of the time of arrival, other parameters of the signal envelope are sometimes measured; at this juncture, this information is stored but is not used as part of the detection or analysis. The duration of a leak detection test is typically 1 h. All of the source locations estimated from the threshold exceedances during a test are used to determine whether the tank is leaking or not. While the algorithms used for detection differ slightly, a leak is declared if a large number of hits are closely clustered in one or more locations. Visual interpretation of the graphical display by the operator has been the most frequent method of analysis. Recently, some of the testing services have begun using a statistical approach to display the number of hits in predetermined areas within the tank.

Figure 2 presents the results of a leak detection test published in Miller[4]. The data from the entire 60-min test is shown in Figure 2(a) and the data from three different 10-min portions of the test are shown in Figures 2(b) - (d). The clustering of data in Figure 2(c) suggests the presence of a leak. This clustering is not observed in the other four 10-min periods (of which only one is shown). It is argued in Miller[4] that the reason why the signal occurs primarily in only a few of the 10-min periods is that the impulsive signals produced by the leak do not occur uniformly in time; however, no evidence is presented to support this argument. The large number of false source locations observed in Figure 2 is also representative of the test data collected by other testing services using a wide-aperture array. The analysis presented in Section 5 offers a probable explanation for the large scatter in the estimated source locations.

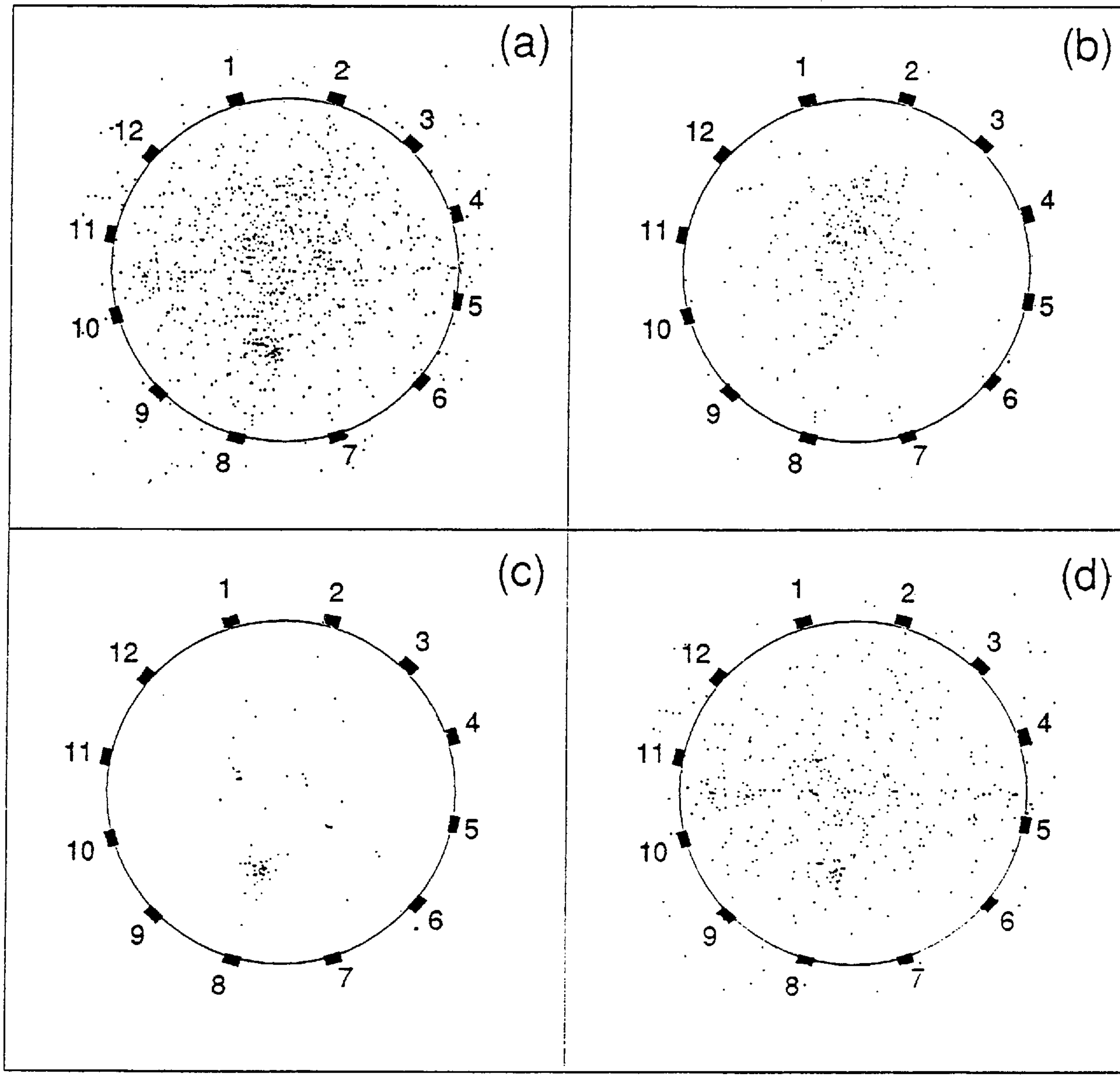

Figure 2. Results of a 1-h leak detection test. Each display shows the location of each threshold exceedance. A clustering of hits indicates the possible location of a leak. Display (a) shows all hits obtained during the 1-h test, and (b through d) show the hits during three separate 10-min periods.[4]

Experiments in a 10-Ft-Diameter AST

DNV Industrial Services provided data from a variety of experiments conducted in 1989 in a 10-ft-diameter, open-top AST that was specially assembled in an asphalt parking area for these tests. The tank, approximately 10 ft in height, was filled with water to a level of approximately 9 ft. It was located on a thick layer of river-sand backfill that was contained by a square wood frame. All of the data analyzed were from experiments in which the tank had a 2-mm-diameter hole in its floor. The water released during the experiments freely drained through the backfill and onto the parking lot. Between experiments, the hole could be plugged from the top of the tank. However, no data were provided on this tank when it was in a nonleaking state, precluding a control analysis. The results of two experiments are presented below. The first experiment compares the time series of the acoustic return simultaneously received from an acoustic sensor mounted on the external steel wall of the tank and one suspended in the water near the top of the tank. The second experiment illustrates the detection capability achieved by a three-dimensional array suspended in the water.

All of the data provided by DNV consisted of time series obtained with a multi-channel transient recorder. Once the threshold established at the beginning of the test was exceeded at any sensor, a 1- to 10-ms time series was recorded and stored for later analysis; the initial threshold exceedance was included in the recorded time series.

Internal Sensor vs. External Sensor Response to a Leak

Time series of pressure fluctuations measured by an internally suspended hydrophone (BK-8105) and an externally mounted resonant sensor were analyzed in an attempt to identify the acoustic leak signal due to the presence of a 2-mm-diameter hole and to estimate the leak's location within the tank. Tank geometry and sensor positions are shown in Figure 3; the

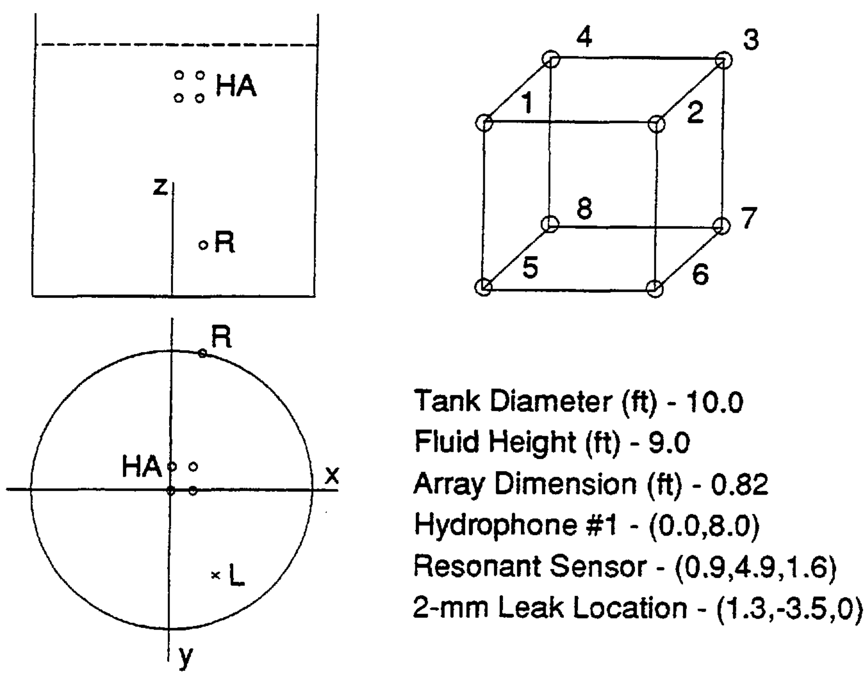

Figure 3. Geometry of the acoustic sensors in the 10-ft-diameter tank.

hydrophone for this experiment was located in approximately the same place as element number 1 of the hydrophone array (HA), while the resonant sensor was located on the outside tank wall at position R. Figure 4 shows time series recorded by both the internal and external sensors. A time-of-arrival analysis with respect to the primary pulse (P) indicates that the observed signal most likely originated near the site of the 2-mm hole. The appearance of this impulse in both the internal and external traces shows that the strongest signals are propagated through the fluid rather than through the tank shell. The relatively small impulse which appears near the t = 2.0 ms time in the external trace is believed to be the leak signal propagated to the sensor via the tank shell. The delay time between this impulse and the primary impulse is consistent with the difference in sound velocity between steel and water (approximately 5,000 m/s as compared to 1,500 m/s). The internal hydrophone receives a secondary impulse (S) delayed by approximately 0.25 ms relative to the primary signal. An analysis of multipath propagation for this particular leak site shows that the time delay of the secondary impulse is consistent with reflections of the acoustic signal from the tank's side wall and/or the fluid surface. The two sources of multipath are shown in Figure 5; the difference in the arrival times for each of these two reflected paths is approximately 0.02 ms, which is not discernible in the time series shown in Figure 4.

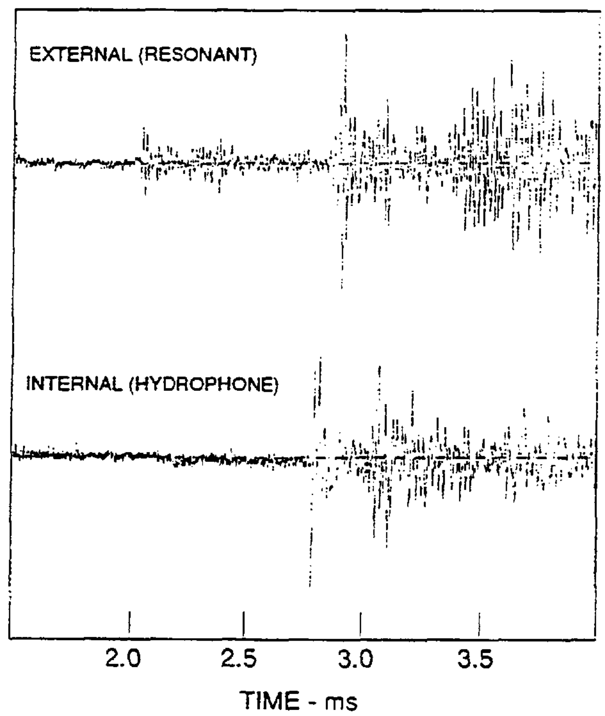

Figure 4. Response of the acoustic sensor mounted on the external shell of the steel tank and the acoustic sensor suspended near the top of the tank. Both sensors are approximately 10 ft from the leak.

Several conclusions may be drawn from the data:

- The impulse arrival time is consistent with a signal emitted from the site of the leak.

- The strongest signals are propagated through the fluid, and a weaker signal is observed to propagate through the tank shell.
- Under relatively quiet conditions in a small tank, externally mounted sensors should be as effective as internal sensors in receiving impulsive leak signals.

Three-Dimensional Internal Array

The hydrophone array used by DNV consisted of eight broadband acoustic sensors located at the corners of a cube with elements spaced at approximately 25 cm. The array was positioned along the center axis of the tank at a height of approximately 8 ft from the tank floor. A 2-mm-diameter hole located at coordinates (1.3 ft, -3.5 ft, 0.0 ft) was open throughout the measurement period (see Figure 3). Figure 6 shows a typical data record obtained during a 1-ms interval within which a large-amplitude event was recorded on seven of the array elements. In

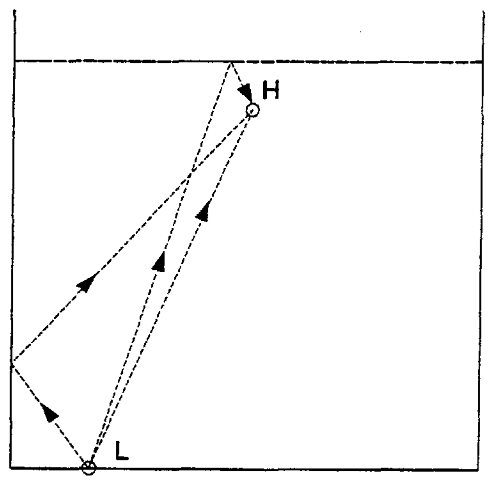

Figure 5. Multipath signals received by the internal array. Both paths have approximately the same time of arrival.

order to estimate the source location corresponding to the primary impulse, the relative arrival time of the impulse was estimated for each of the time series shown. Combining the measured arrival times with the array geometry and speed of sound, a least squares method of estimation was used to determine the most likely origin for the acoustic impulse. All of the data records analyzed in which the primary impulse is easily identified suggest a leak located near coordinates (1.4 ft, -2.8 ft, -1.3 ft) with a standard deviation of 0.2 ft (Figure 7). The difference between the predicted source location and the actual leak site cannot be accounted for by a simple adjustment in sound speed. It is believed that the small array size coupled with an inexact knowledge of array dimensions and orientation is consistent with the error in the predicted source location.

A secondary impulse, occurring approximately 0.3 ms after the primary impulse, is clearly visible in six of the array element time series. The secondary signals occur as a result of reflections of acoustic impulses from the tank wall or air/water interface. An analysis of the expected arrival times of impulses reflecting off of the tank's side-wall or off of the air/water interface above the array shows that the particular secondary signals observed in DNV's data are most likely due to reflections off the tank's side-wall. Though not attempted thus far, it should be possible to use the relative arrival times between secondary impulses to compute a second, independent estimate of source location within each data record.

Interpretation of the Results

These tests clearly illustrate the existence of a signal produced by a leak and show that this signal propagates both through the steel walls of the tank and through the water. The signal that propagates through the water is much stronger than that which propagates through the wall. The experiments also show the primary propagation path (i.e., the direct path from the leak to the sensor), the discrete multipaths (i.e., the leak-wall-sensor path and the leak-surface-sensor path), and the reverberation. Registering these signals and correctly identifying the same signal in each sensor is important to the detection scheme. Due to gain peaking near the sensor cutoff frequency, the DNV time series provide no information as to the spectral content of the leak signal at high-frequencies; furthermore, at approximately 1 ms, they are too short for any low-frequency analysis. Nevertheless, there is no doubt that the data collection scheme and signal analysis employed are adequate for locating single leaks within a small storage tank. However, no background noise data were collected during these experiments, so the strength of the signal relative to the background level is unknown. Neither did these experiments give any insight into the source mechanism(s) which give rise to the acoustic leak signal.

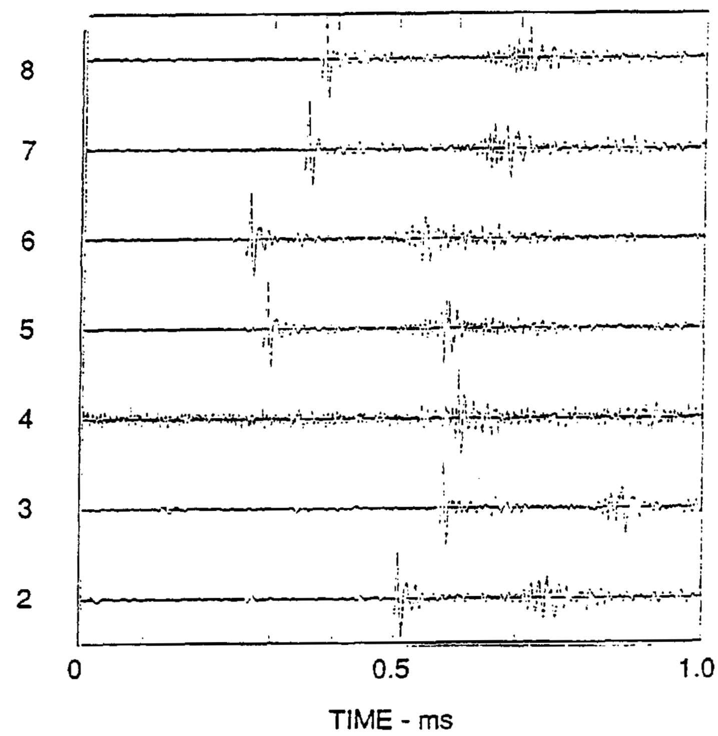

Figure 6. A 1-ms time series obtained from seven of the eight sensors mounted on the internal array suspended in the tank. The data were taken at a 1-MHz sampling rate.

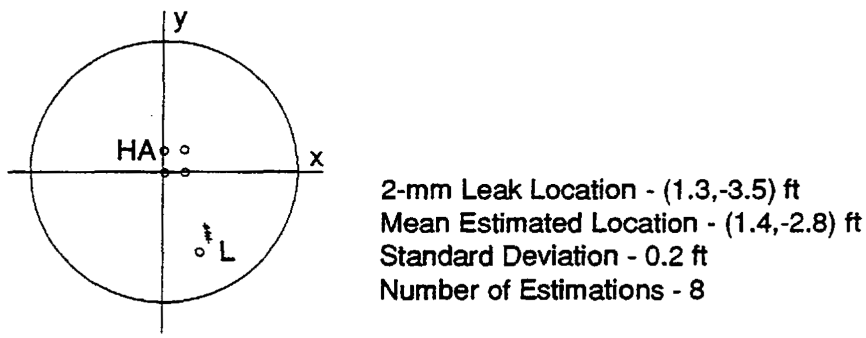

Figure 7. Location of the seven independent hits made with the internally suspended acoustic array; one of the eight sensors on the array was not working properly during the experiment.

Laboratory Experiments

The design of a passive acoustic leak detection system for use in ASTs, including both sensor specification and signal processing strategies, is determined largely by the nature of the signal to be detected and the background noise field within which the system must operate. As mentioned in the Introduction, few papers have been published concerning the characteristics of the leak signal or the mechanisms by which leak signals are produced. Because of previous work done in the field of acoustic emissions, currently available leak detection systems have been designed under the assumption that the leak signal contains a large, persistent impulsive component. Although impulsive leak signals have been observed in several leak-simulation studies, no published data exist to support a theory for the impulse source mechanism. In addition, the possibility that non-impulsive leak signals may be exploited for the purpose of leak detection has been largely ignored by the industry.

This section describes a set of laboratory experiments designed to answer some basic questions regarding the character of the leak signal produced in an AST. The intent of these experiments was to verify the presence of a strong, impulsive component in the leak signal and to determine whether a low-frequency signal is also present. A leak simulator was constructed to allow flexibility in the choice of flow rate, backfill material, and drainage conditions. Three distinct types of leak signals were observed: impulsive, broadband, and low-frequency. The conditions under which these simulated leak signals are produced are discussed below.

After a brief description of the experimental apparatus and procedure, data will be presented in which the different leak signal components are present. Air bubbles interacting with the flow field, particulate collisions with the tank bottom, turbulent flow noise, and cavitation will be explored as possible mechanisms by which the various leak signal components may be produced.

Experiment Design

Figure 8 shows a diagram of the leak simulator used in the experiments. The apparatus is constructed of 10-cm-diameter PVC tubing and houses two HSBIT-30 acoustic sensors. Sensor positions relative to the leak aperture are 10 cm (near-field) and 125 cm (far-field). The acoustic signals were amplified with Panametrics 5660C preamplifiers and anti-alias-filtered within a Western Graftec TDA-3500 transient data recorder. The HSBIT-30 sensor combines reasonable low-frequency sensitivity with a sharp resonance near 25 kHz. Thus, both impulsive and broadband leak signals can be captured at a relatively low sample rate of 50 kHz. At this sample rate, the TDA-3500 is capable of recording a time series of 84-s duration (2 Msamples). The backfill material into which the leak impinged consisted of various combinations of water, fine-grain beach sand, and pea-gravel. In order to simulate different drainage conditions, drain lines were installed near the water/soil interface and at the bottom of the backfill basin. Flow rates of approximately 20 gal/h were generated through a 3-mm-diameter circular aperture. A storage reservoir was positioned above the simulator to allow a constant pressure head of up to 180 cm to be maintained for indefinite periods during which the leak was active.

Data

Figure 9 shows three different backfill combinations used to investigate the leak signal and source mechanisms. The flow of fluid into the backfill material of an AST eventually creates a cavity below the leak aperture. In order to simulate this effect, a gap (typically 1 to 2 cm) was placed between the simulated leak and the backfill surface. Pressure fluctuations within the turbulent flow field produced by the leak will contribute to the acoustic leak signal. This source mechanism is best isolated by using a water backfill, though the sound of turbulent flow should be apparent under any backfill condition. The effect of air entrainment into the leak's flow field, and of particulates striking the tank bottom, was investigated through the use of soil backfills. Because of their consistency (in terms of particle size) and similarity to the type of clean backfills typically found beneath ASTs, fine-grain sand and approximately 3-mm-diameter pea-gravel were chosen as soil backfill materials. The data recorded for a given backfill and pressure head consisted of eight 1.3-s-long time series of pressure fluctuations obtained over a period of up to 1 h of continuous operation. In addition to the eight time series recorded while the leak was active, a time series was obtained at full pressure head with the leak closed. This allowed a comparison to be made between the leak signal and the background noise level.

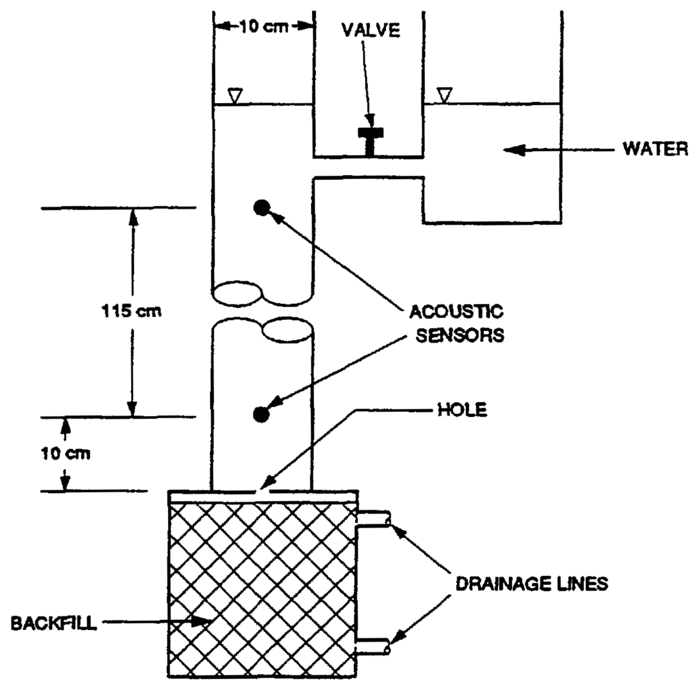

Figure 8. Leak simulator design. The containment tube is constructed from 10-cm-diameter PVC tubing. The acoustic sensors are HSBIT-30 frequency-selective sensors. The maximum pressure head applied during the experiments was 180 cm of water.

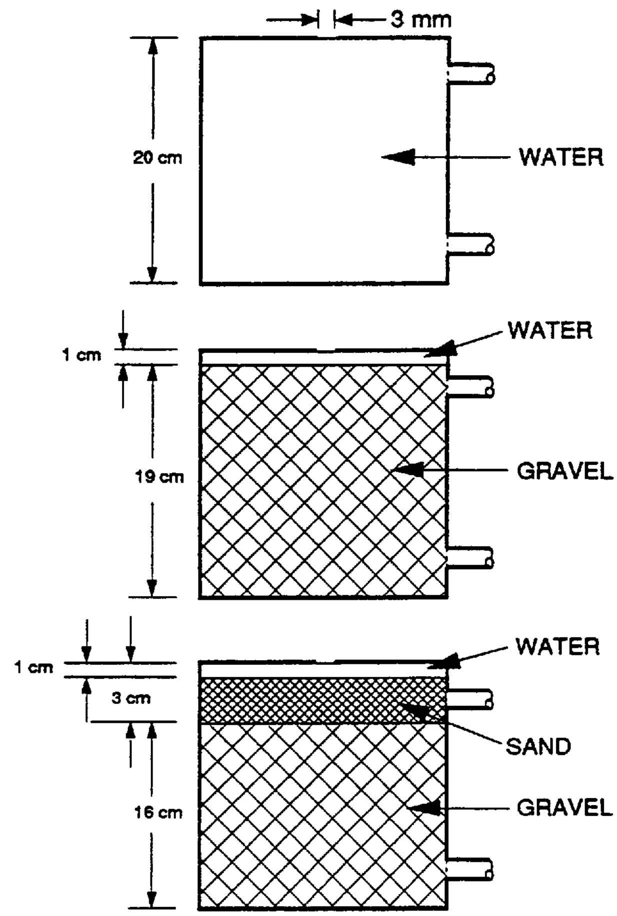

Figure 9. Backfill configurations used in the simulator experiments.

Figure 10 shows time series of acoustic signals received by the near-field sensor for the three different backfill configurations after all air bubbles had been expelled from the backfill material (full saturation). The complete expulsion of air bubbles was verified by two methods: listening for the end of impulse production by monitoring the audio portion of the HSBIT-30 output through a remote speaker, and disturbing the backfill material with a probe to force the release of trapped air bubbles. In Figures 11 through 13, power spectral density plots for these time series are presented. In each case the pressure head was 170 cm and the diameter of the aperture was 3 mm. The measured flow rate for these experiments was approximately 20 gal/h. At this flow rate the average fluid velocity near the leak aperture was approximately 3 m/s. Figures 12 and 13 contain similar data obtained in the presence of air bubbles entrained into the leak flow field (partial saturation). Soil backfills naturally expel air bubbles for some time after the initiation of a leak. With water as the backfill material, isolation of the air bubble/flow-field interaction as a source mechanism was done by artificially introducing air beneath the leak by means of a syringe.

The sample rate used to collect each of the six data sets was 50 kHz. Power spectral density plots represent an average of 31 2048-point FFT's individually detrended and weighted with a cosine bell. Other than the initial anti-alias filter, no filtering was applied to the time series data.

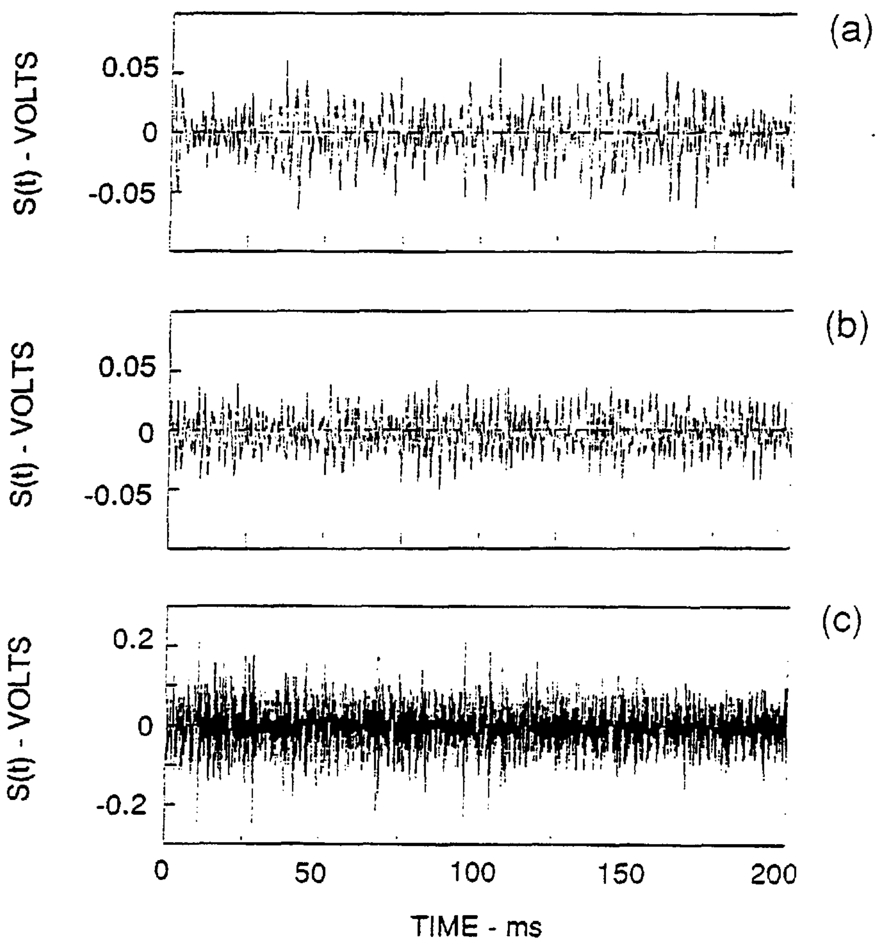

Figure 10. Time series of the pressure fluctuations recorded with the near-field sensor when air bubbles are not present in the backfill. Backfill materials are (a) water, (b) gravel, and (c) sand.

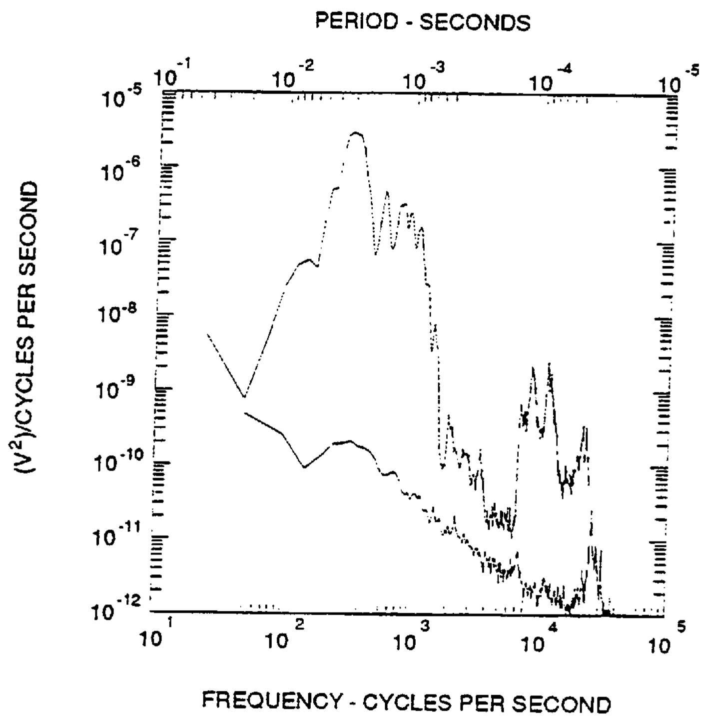

Figure 11. Power spectral density of the pressure fluctuations recorded with the near-field sensor. The backfill material is water; air bubbles are absent. For reference, the spectrum is also shown when no leak is present.

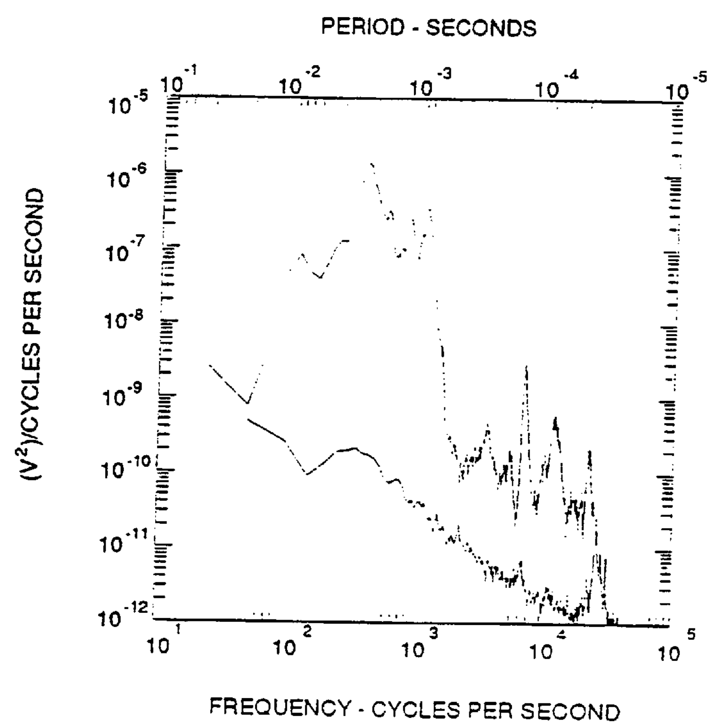

Figure 12. Power spectral density of the pressure fluctuations recorded with the near-field sensor. The backfill material is gravel; air bubbles are absent. For reference, the spectrum is also shown when no leak is present.

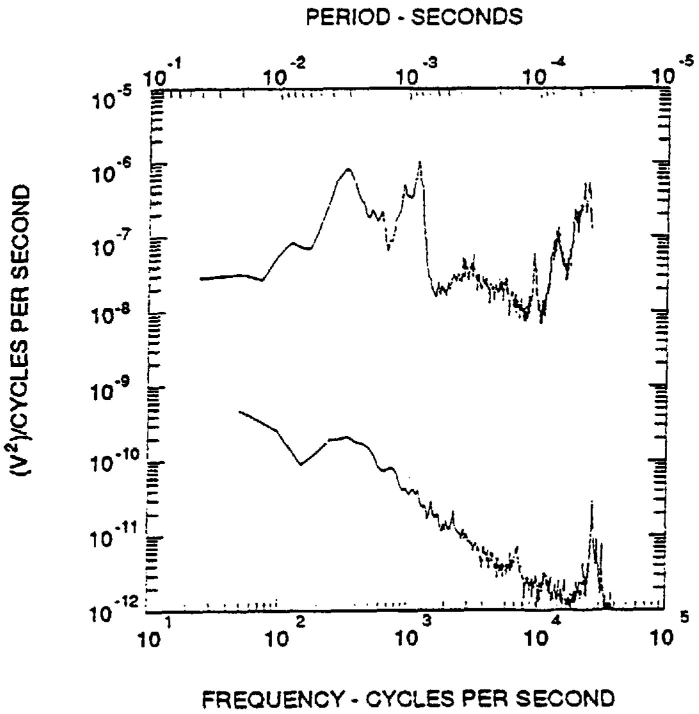

Figure 13. Power spectral density of the pressure fluctuations recorded with the near-field sensor. The backfill material is sand; air bubbles are absent. For reference, the spectrum is also shown when no leak is present.

Analysis

The most striking feature of the six time series is the presence of large-amplitude impulses that dominate the partial saturation data (Figure 14). These impulses were observed only during experiments in which air bubbles were allowed to interact with the leak flow field. Impulsive signals induce a resonant response in acoustic sensors. This response may be viewed either as a brief ringing at the sensor resonant frequency (time series) or a sharp peak at the resonant frequency (power spectra). Spectra computed during periods of partial saturation all contain sharp peaks near the f = 25 kHz HSBIT-30 resonant frequency (Figure 15 through 17). If the leak signal is confined within a cavity, a resonant response associated with the dimensions of the cavity may also be induced. Spectral peaks at f = 0.4 kHz and f = 10 kHz represent the response of the containment column and backfill basin to the impulsive leak signal. In an AST, the impulse-induced containment-column resonance occurs at a much lower frequency (due to the large AST dimensions) and will most likely be undetectable against the background noise level. Under certain backfill conditions, however, the backfill-cavity resonance observed in the simulator experiments may be detectable, and can be considered as part of the leak signal. In addition to the resonant response, a broadband rise in spectral energy occurs as a result of the short duration of impulse signals. Because the volume of soil contained in the backfill basin was small (approximately 3.5 l), the impulsive signal did not persist over a long period of time. The time scale over which the impulses disappear is relatively short for gravel (approximately 5 min) but is much longer for fine-grain sand (approximately 1 h). For all three backfill conditions, experiments were performed in which the impulsive signal was allowed to decay completely, and then a small quantity of air (approximately 1 cc) was injected near the leak aperture. Upon injection of the air, the impulsive component of the leak signal immediately reappeared and persisted for periods of up to 1 minute. Due to their granular nature, soils allow the entrapment of a great deal of air within the space between sand or gravel particles. Once wetted, this air tends to percolate upward through the soil. In the presence of a leak, which produces regions of low pressure due to the high fluid velocity and turbulent nature of the flow, some of this air is entrained into the flow field. Due to the compressibility of air, stresses transmitted from the flow to the air bubbles result in relatively large pressure fluctuations. Pressure fluctuations associated with bubbles, occurring on short time scales, produce impulsive sounds.

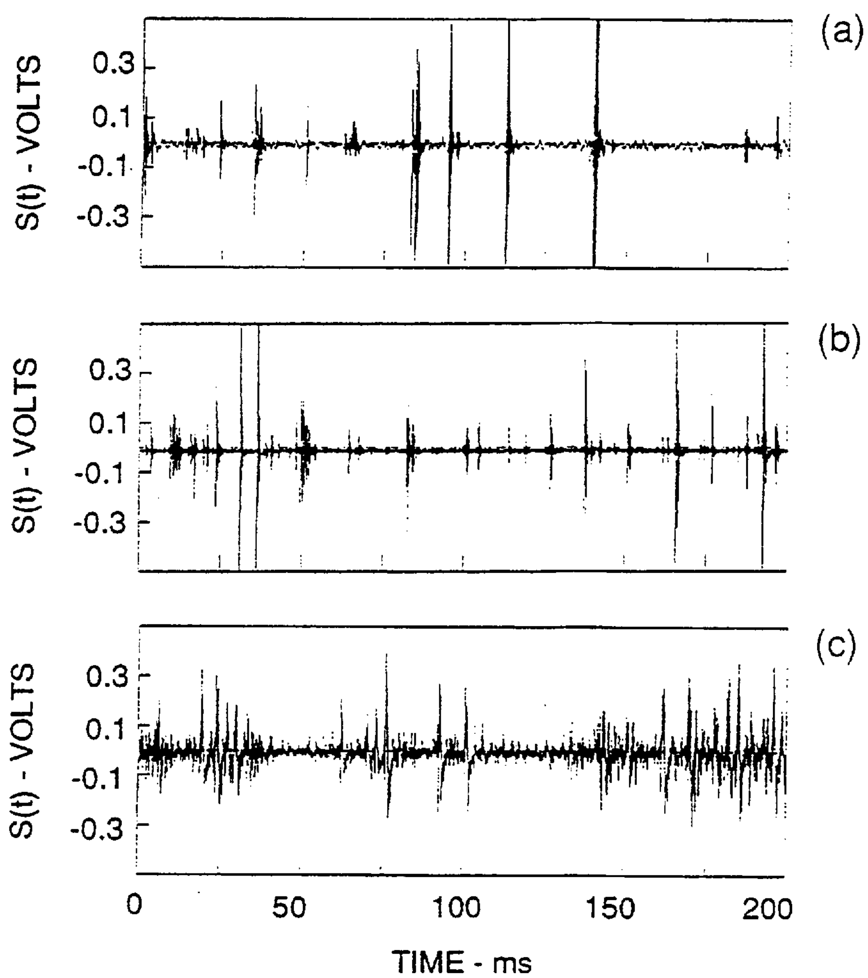

Figure 14. Time series of the pressure fluctuations recorded with the near-field sensor when air bubbles are present in the backfill. Backfill materials are (a) water, (b) gravel, and (c) sand.

Cavitation was also explored as a mechanism by which the impulsive leak signal may be produced. The lack of cavitation near the leak aperture was verified by using water as the backfill material. In the absence of bubble-induced impulses and tank bottom/particulate collisions, no acoustic signal due to cavitation was observed. If the leak is treated as similar to a circular orifice placed within a hydraulic pipeline, theoretical predictions of the flow conditions (pressure head, leak diameter, etc.) necessary to initiate cavitation can be made. These calculations indicate that cavitation should not be expected at a pressure head of 2 m. Pressure heads greater than 10 m may, however, be sufficient to cause cavitation. The existence of cavitation as an AST acoustic-source mechanism, and the nature of the sound produced by cavitation near a leak, should be evaluated through further field experiments.

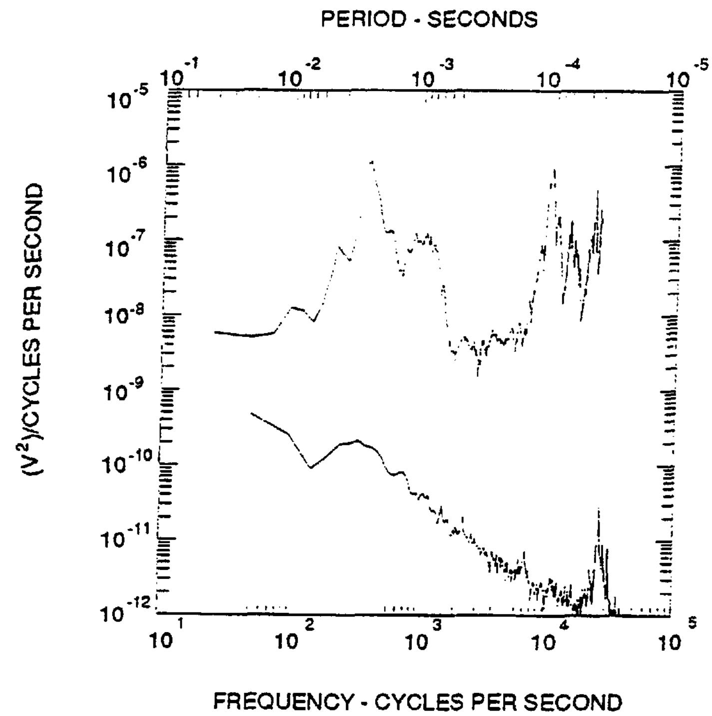

Figure 15. Power spectral density of the pressure fluctuations recorded with the near-field sensor. The backfill material is water; air bubbles are present. For reference, the spectrum is shown when no leak is present.

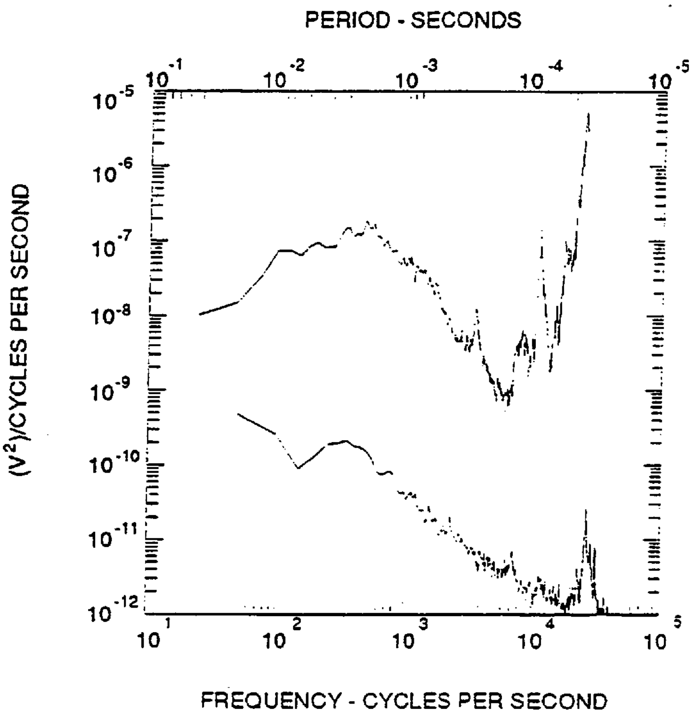

Figure 16. Power spectral density of the pressure fluctuations recorded with the near-field sensor. The backfill material is gravel; air bubbles are present. For reference, the spectrum is shown when no leak is present.

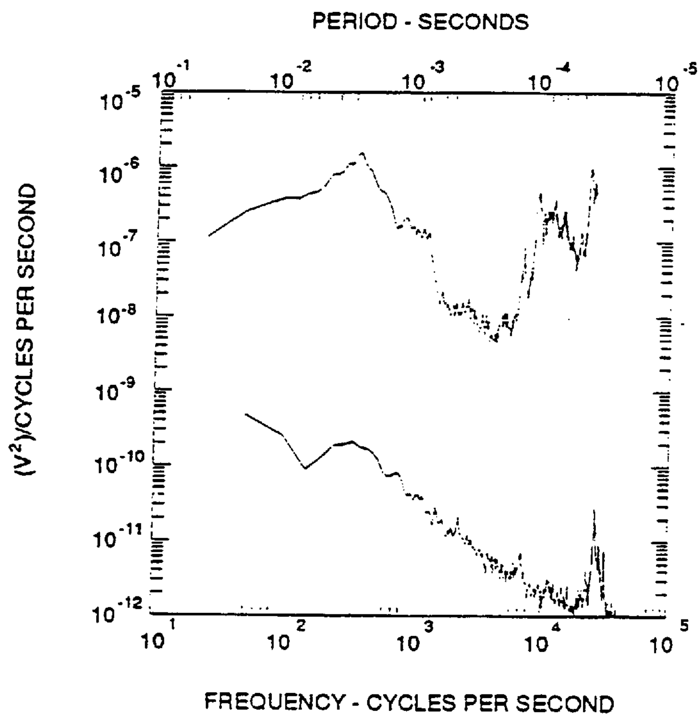

Figure 17. Power spectral density of the pressure fluctuations recorded with the near-field sensor. The backfill material is sand; air bubbles are present. For reference, the spectrum is shown when no leak is present.

A second, less energetic type of impulsive sound was observed by placing a layer of saturated sand below the leak aperture (Figure 9(c)). The effect of the sand layer is to produce a broadband rise in spectral energy level (Figure 13). The generating mechanism for this component of the leak signal is believed to involve the collisions of sand particles with the simulator floor. Though this signal is termed impulsive due to the generating mechanism (collisions), the high rate at which collisions occur and the relatively small amount of acoustic energy given off per collision create a signal which is similar to white noise in both the time and frequency domain. In contrast to the signals recorded in the presence of air bubbles, impulses that greatly exceeded the average signal level were not observed for leaks into fully saturated sand.

The sound of turbulent flow through the leak aperture contributes to the low frequency (DC to 2 kHz) acoustic leak signal under all backfill conditions. This effect is most evident in the power series where a substantial difference in signal level is observed between the active-leak and zero-leak data. Neither the amount by which this signal is attenuated over typical AST dimensions nor the level of AST background noise at low frequencies has been fully investigated, although some work has been done by Chevron Oil Field Research[5]. An estimate of the upper frequency scale of turbulent flow noise can be made from the diameter of the aperture and the velocity of the fluid at the aperture. Using the measured flow rate of 20 gal/h, a 3-mm-diameter hole should have an upper frequency scale (v/D) of approximately 1 to 2 kHz. This is in good agreement with the power spectral density plots, which all exhibit a sharp decrease in energy level near f = 2 kHz.

Discussion

Based upon the leak signals generated by a simulator, it is likely that at least three source mechanisms, each with a unique acoustic signature, will contribute to the leak signal found within an actual AST. The three signals that have been identified are:

- bursting air bubbles (broad-band, impulsive),
- turbulent flow noise (low-frequency, continuous), and
- particulate collisions (broad-band, continuous).

Currently available leak detection systems have been designed under the assumption that a large-amplitude, impulsive signal exists in leaking ASTs. The leak simulation experiments showed that impulsive signals require the entrainment of air bubbles into the leak flow field. While impulsive signals offer the advantage of detectability (due to their large amplitude), the persistence of impulsive signals within actual ASTs has not yet been addressed.

The existence of low-frequency and broadband leak signals, due to turbulent flow noise and particulate collisions, may be important in the design of future leak detection systems. Such signals, though less energetic than impulsive bursts, may be relatively insensitive to changes in backfill and drainage. Detection systems that respond only to impulses view the low-frequency and broadband leak signals as additional noise within which the system must operate. Consequently, the presence of these signals acts to degrade the performance of currently available systems. Should the low-frequency and broadband signals prove detectable over typical AST dimensions, however, a leak detection scheme exploiting all three components of the leak signal could be designed. A leak detection system based on the presence of a continuous signal would allow the application of more reliable signal processing algorithms to the detection/location problem.

The acoustic signal observed within a given AST will be influenced by many conditions: backfill material, leak shape and size, pressure head, etc. This experimental study cannot predict what sort of acoustic signal a particular leak will produce, but instead draws attention to a variety of possible source mechanisms. Which of these signals offer the best hope of being reliably detected and located can only be determined through field experiments, preferably conducted in the presence of real (as opposed to simulated) leaks.

Assessment of Current Acoustic Methods

The testing services base their detection systems on the presence of large, distinctive, impulsive signals produced by a leak. While the laboratory experiments demonstrate that such signals exist, they also suggest that bubbles are the only mechanism that will produce the type of impulsive signals that are detectable given currently used data collection and data analysis schemes. The persistence of these signals in the field is unknown. The laboratory experiments show that entrainment of air in the backfill is necessary for these signals to persist over time. Because of the configuration of the backfill under the 10-ft-diameter tank, the experiments almost guarantee that such signals will persist. The backfill will never saturate, because it is free to drain; thus, the laboratory tests suggest that detectable impulsive events should occur. The laboratory tests also suggest that there are two other mechanisms that should produce detectable signals. However, these signals require coherence analysis using the time series of the data, and none of the testing services have attempted to exploit this type of signal.

This section presents a discussion of the effectiveness of the approach currently being used for detection. First, a simple analysis of the data collection scheme is presented. This analysis is intended to determine the impact on performance of acquiring signals from different acoustic impulsive events. This *impulse-mixing* analysis assumes that strong impulsive signals exist during the entire leak detection test and that only the signal that directly propagates from the leak to the sensor (i.e., primary signal) exceeds the threshold. (In practice, there are many threshold exceedances that occur that do not result from the primary signal. These other threshold exceedances are associated with multipath, reverberation, noise, etc.) A discussion of the threshold level and the element spacing in the sensor array follows this analysis.

Impulse-Mixing Analysis

Figure 18 illustrates the time of arrival of only primary impulsive signals at four sensors equally spaced around the circumference of a tank. It is assumed that sensor 1, s_1, is closest to the leak and therefore receives the signal first. This signal, plus the next threshold exceedance on each sensor, is called an arrival time data set t_{ijk}, where t is the arrival time for sensor i, acoustic event j, and data collection period k. Three impulsive signal events and two data collection periods are shown to illustrate the problem. The first data collection period, consisting of the sampling period τ_c and the waiting period τ_r for reverberation and multipath to subside, records only acoustic signals from the first event. The second data collection period, however, includes signals from two different acoustic events. In this case, the first impulse is not received by sensor 1. Instead, the first impulse is received by sensor 3. This impulse then triggers the collection of the arrival data set for data collection period 2; this second data collection period contains impulses from acoustic events 2 and 3. The second data collection arrival set will not accurately locate the source of the leak. Analysis of this arrival time data set will lead to a false location and may be the cause of much of the scatter observed by the testing services.

Mixing of impulses will occur if the frequency of the primary signals due to a leak is high enough, (i.e., if they occur more frequently than $(\tau_c + \tau_r)^{-1}$). This mixing of impulsive signals from different acoustic events occurs because the data collection system is turned on and off. When the system "wakes up," there is no way to determine which group of signals is occurring, and as a consequence, there is a chance that the arrival time set consists of an unwanted mixture of signals.

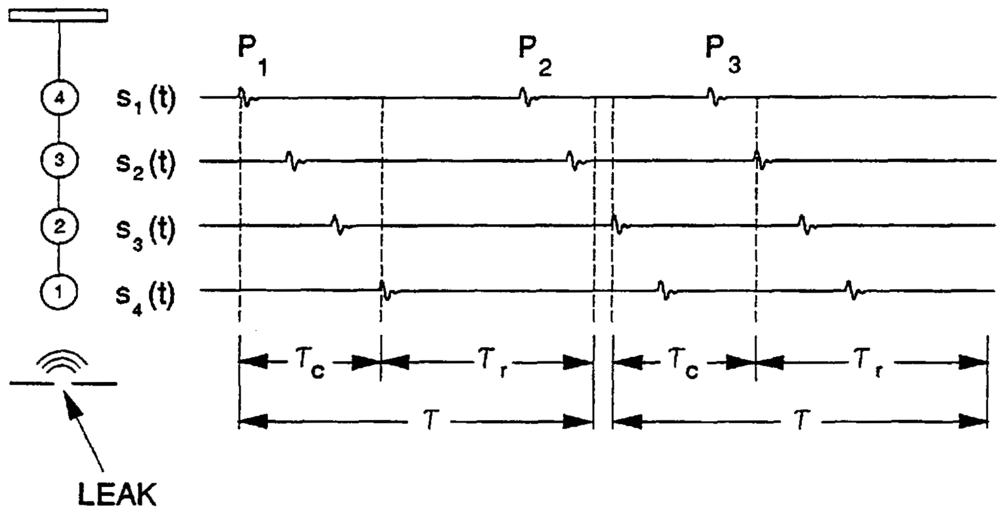

Figure 18. Impulsive acoustic return from five sensors for two data collection periods.

The probability of receiving a contaminated data set is estimated below. It is assumed that the impulsive signal events occur randomly and that the probability of occurrence of these impulsive signals is Poisson distributed. This distribution is typically used to simulate the arrival time of discrete events. The probability $P_n(\tau)$ that an impulsive signal is generated during the observation time period $\tau = \tau_c + \tau_r$ is

$$P_n(\tau) = [(f_i\,\tau)^n\, e^{-(f_i\,\tau)}]/n! \quad (1)$$

where f_i = average number of impulsive events per second, $\tau = \tau_c + \tau_r$ = observation time interval, and n = number of impulse events observed. It is assumed that the probability that a mixed arrival time set is collected is equal to the probability that an acoustic event is produced within a time τ after a trigger has been accepted.

The probability that an arrival time set is contaminated $P_{mix}(\tau)$ and is composed of two or more pulsive events is given by

$$P_{mix}(\tau) = 1 - P_o(\tau) = 1 - e^{-(f_i\,\tau)} \quad (2)$$

For a 100-ft-diameter tank and a wide-aperture array with sensors located on the circumference of the tank, $\tau = \tau_c + \tau_r \cong D/c + 2\,D/c$ = 60 ms, where D is the diameter of the tank and c is the speed of sound in the product. By solving Eq. (2) for f_i, the number of impulsive events can be estimated for a desired $P_{mix}(\tau)$. For t = 60 ms, only 12 impulsive events per second are required for 50% of the sample sets to be contaminated.

The validity of this analysis was checked with the laboratory data collected with both sand and gravel backfills. Several of the long time series collected in the laboratory were analyzed to estimate the number (i.e., frequency f_i) of primary impulses received during a 1-s period. A simple count of only the very strongest impulses based on a visual examination of the data showed as many as 40 to 50 events per second. This number would dramatically increase if threshold settings typically used by the testing services were used. This suggests that the probability of having a contaminated data set is over 90%. This probability is even higher if threshold exceedances due to acoustic energy other than that of the primary signal are included. The validity of assuming a Poisson distribution was also checked. A statistical hypothesis analysis showed that the cumulative frequency distribution of the threshold exceedances was not statistically different from a Poisson distribution at a level of significance of 5%.

Recommendations for Minimizing Impulse-Mixing

The current method of collecting data tends to enhance the probability of collecting a contaminated time-of-arrival data set. First, the thresholds that are typically used are too low. As a consequence, threshold exceedances from other than the strongest primary signals trigger the collection of a time-of-arrival set. The data collected in the laboratory suggest that a higher threshold should be used and that if used, more than an adequate number of impulsive events would be detected. In fact, the number of strong acoustic events occur too frequently for the data collection scheme being used, and contaminated data sets are almost assured. Second, the on/off data collection scheme is a primary contributor to the collection of contaminated data sets. A more advanced data collection scheme is required if the number of contaminated data sets are to be minimized. Third, the large spacing between sensors in the wide-aperture arrays also results in a higher probability of contaminated data sets, because the time of arrival between receiving the primary signal at each sensor is long. During this time period, other unwanted threshold exceedance could occur. The advantage of using a narrow-aperture array is best illustrated by the acoustic return shown in Figure 7. Fourth, a signal processing scheme needs to be developed that addresses both the portion of the signal being detected and the characteristics of the noise. This signal processing scheme needs to follow a more comprehensive set of rules to distinguish noise-derived hits from leak-derived hits. Regardless, it is recommended that a continuous time series be collected. The laboratory experiments suggested that sample rates between 50 and 100 kHz will suffice. A more detailed analysis of the signal processing can not be discussed until the characteristics of the noise are better defined. The nature of the ambient noise will be investigated in the upcoming field tests in the 117-ft-diameter tank.

The impulse-mixing analysis offers a plausible explanation for the large scatter (i.e., large number of false alarms) observed in the data obtained by the testing services (see Figure 2). If this explanation is correct, then changes to the data collection, sensor geometry, and signal processing currently being used are required if the number of false hits is to be reduced and the number of hits due to a leak increased.

Conclusions

There are a number of important observations, conclusions and recommendations that can be made from the analyses presented in this paper. First, a leak signal exists, and it is much stronger than the nonleak signal. Three distinctive signals were observed in the laboratory experiments: (1) an impulsive, high-frequency signal that is apparently generated by the collapse of bubbles in the vicinity of the leak, (2) a low-frequency signal produced by the turbulent flow through the hole, and (3) a broad, high-frequency response due to the noise generated by particulates striking the tank floor. This last signal has not been discussed in the literature. The strength of these signals is dependent on the flow rate, the nature of the backfill, its composition, the degree of saturation and drainage, and the extent of the erosion of the material beneath the hole. Only the impulsive signal is being exploited by the commercial leak detection testing firms. The laboratory data suggest that the other two signal sources are as strong as the impulsive signals.

Second, the experiments conducted in the 10-ft-diameter AST suggest that an acoustic signal produced by a leak does exist and that its main propagation mode is through the product. The experiments further suggest that the signal received with a sensor mounted to the external wall of the tank is as strong as that received by a sensor mounted in the tank. A signal produced by the leak was also observed propagating through the steel wall of the tank; however, this signal was much smaller than the signal propagating through the product. The advantages of having closely spaced sensors with vertical elements is clearly illustrated by the data collected with the three-dimensional internal array. These data were taken expressly so that the impulsive signal could be investigated.

Third, there is a high probability of improper time registration of the data being collected to detect the large-amplitude leak signals. These problems occur because of the on/off approach to data collection and the use of low thresholds; they increase when wide-aperture sensor arrays are used and when there are no vertical sensor elements. Time registration problems occur when the impulsive signal generated by a leak at any point in time is not the same impulsive signal that is received at one or more of the other sensors in the array. Impulse mixing can occur from the mixing of impulsive events from the same leak or two or more leaks, from the mixing of an impulsive event from a leak and the multipath or reverberation of a previous leak signal, from the mixing of an impulsive event from a leak and external noise, or from noise. To minimize these time registration problems, better data collection, sensor configurations, and signal processing are required.

Fourth, while the laboratory data suggest the presence of three signals, field data collected in a tank with a known leak must be obtained if one is to determine which signals actually occur and persist in the field and how strong they are. In addition, the attenuation of these signals is not presently known, but an assessment can be made in the experiments being planned for the 117-ft-diameter tank in the near future.

Fifth, the noise field needs to be characterized to develop signal processing schemes and to make an estimate of performance. The field tests on the 117-ft-diameter tank will attempt to make an estimate of the background noise.

Sixth, most of the data collected to detect the large-amplitude leak signals are sampled at a very high rate. The laboratory data suggest that this is unnecessary. While the sampling rate will be a function of which portion of the signal produced by a leak is being exploited, a sample rate of less than 100 kHz is more than sufficient. While not discussed in this paper, the high-frequency broad band and the impulsive realizations of the signal do not appear to be enhanced in any particular frequency band. This will allow longer time series to be collected and analyzed.

Seventh, there is high potential for use of this technology for leak detection, but changes appear necessary to achieve this potential. Fortunately, this need has been anticipated by the commercial companies, as they are in the process of implementing new data acquisition systems capable of digitally collecting long continuous time series for data processing. Unlike conventional acoustic emissions technologies in which an emission is a very infrequent event, the laboratory data suggest that the leak signal is always present.

The experiments planned for the 117-ft-diameter tank will investigate different data collection schemes, different array configurations (wide versus small aperture, internal versus external arrays), and different signal processing schemes. These experiments will focus on determining the nature of the background noise.

A detailed discussion about the advantages and disadvantages of internal versus external arrays is premature. This comparison should await the completion of the field tests in the 10-ft- and 117-ft-diameter tanks. The data obtained so far suggest that the signal level is about equal for both types of detection schemes. What is not known is the background noise level. Both the internal and external arrays are subject to the same type of multipath; however, the internal should be able to better distinguish the various propagation paths. Operationally, it is preferred that the sensors be attached to the external wall of the tank. This results in better geometric control, safer operations (no one has to climb to the top of the tank to lower the sensor into it), and does not require the sensors to be liquid-tight. Unlike the internal sensors, however, the external sensors will be subject to external sources of noise, especially man-made noise. This noise is sensed on the backside of the sensor. Unless the external sensors have sufficient isolation, the acoustic signals that occur in the tank will be contaminated with this additional source of noise. Experiments in a 10-ft-diameter tank are in progress to investigate this noise source.

The analytical and experimental work completed to date is very encouraging and suggests that a passive acoustic leak detection system can be used to detect small leaks in ASTs. These experiments suggest that a detectable signal does exist, but the approach to data acquisition and signal processing needs to be improved in order for the technology to achieve its full potential.

Acknowledgments. The authors are especially grateful and would like to thank and acknowledge DNV Industrial Services, Inc., for providing the raw acoustic data from the 10-ft-diameter AST experiments for analysis and to Hartford Steam Boiler Inspection Technologies, for supplying the acoustic transducers and preamplifiers used in the collection of the laboratory data. This work was funded by a contract with the American Petroleum Institute. The authors would also like acknowledge the encouragement and technical review provided by the API Task Force monitoring this work.

References

1. Starr, J. W., and J. W. Maresca, Jr., "Leak Detection Technologies for Aboveground Storage Tanks When In Service," Final Report, American Petroleum Institute, VistaResearch Project 2032, Vista Research, Inc., Mountain View, California (August 1989).

2. Maresca, J. W., Jr. and J. W. Starr, "Aboveground Tank Leak Detection Technologies," in *Proceeding of the Tenth Annual OLTA Operating Conference*, Houston, Texas (June 1990).

3. Nickolaus, C. M., "Acoustic Emission Monitoring of Aboveground Storage Tanks," *Materials Evaluation* (March 1988), pp. 508 - 512.

4. Miller, R. K., "Tank Bottom Leak Detection in Above Ground Storage Tanks Using Acoustic Emission," in *Proceedings of the Conference on Above Ground Storage Tanks*, Center for Energy and Environmental Management (8-9 November 1989).

5. Chevron Oil Field Research Company, "Detection of Leaks in Petroleum Storage Tanks Using Geophysical Techniques," Technical Report, Chevron Oil Field Research Company, La Habra, California (28 August 1987).

Appendix B

Field Tests of Passive Acoustic Leak Detection Systems for Aboveground Storage Tanks When In Service

E. G. Eckert and J. W. Maresca, Jr.

Vista Research, Inc.
Mountain View, California

Field Tests of Passive Acoustic Leak Detection Systems for Aboveground Storage Tanks When In Service

Eric G. Eckert and Joseph W. Maresca, Jr.
Vista Research, Inc.
Mountain View, California

10 September 1991

Abstract

An evaluation of the applicability of passive-acoustic remote sensing techniques to the problem of leak detection in aboveground storage tanks (ASTs) was conducted during a series of experiments on a 114-ft-diameter AST located at the Mobil Oil Refinery in Beaumont, Texas. The primary goals of the experiment were to: (1) investigate the detectability of impulsive and continuous acoustic leak signals, (2) measure the ambient noise field against which the leak signals must be detected, and (3) obtain continuous time series using a variety of sensor arrays so that improved leak detection algorithms can be tested. Simulated acoustic leak signals were generated and controlled through the use of a siphon-operated leak simulator. Data were recorded in the form of time series of acoustic signals using a variety of wide- and narrow-aperture external arrays and a pair of submersible hydrophones.

Impulsive leak signals generated by the interaction of air bubbles with the leak flow field were found to be detectable over the dimensions of the AST. The signal-to-noise ratio for impulsive leak signals, the rate of impulse emission, and the degree to which these signals maintained their similarity over the array aperture resulted in signals that could not be reliably analyzed using acoustic emissions techniques for data acquisition and signal processing.

Continuous leak signals generated by turbulent flow, particulate collisions, and cavitation were found to be detectable over the dimensions of the AST. The signal-to-noise ratio for continuous signals recorded using external sensors was relatively low at frequencies below 10 kHz due to the high level of ambient noise encountered at the refinery.

A beam-forming detection algorithm designed for use with both impulsive and continuous leak signals was developed and applied to data obtained using externally mounted sensor arrays. Source location estimates resulting from the application of the beamforming algorithm to impulsive and continuous data were consistent with the known location of the leak simulator.

Introduction

A leak in the floor of an aboveground storage tank (AST) produces an acoustic signal. If the acoustic leak signal is not significantly different from the ambient noise field, the presence of a leak must be inferred through the process of detection-through-location. Regions of the AST floor that are observed to radiate acoustic energy in excess of a measured background level are interpreted as likely leak locations. The process of constructing a sound-level map of the AST floor presently requires that the acoustic signal be recorded by an array of spatially separated sensors. The quality of a sound-level map obtained through passive-acoustic measurements, and hence the reliability of a passive-acoustic leak detection system, is affected by a variety of parameters: leak signal strength in comparison to the ambient noise, the number and separation of the array elements, the degree to which the recorded signals retain their similarity over the dimensions of the array, the form in which the leak signals are acquired, and the type of processing applied to the recorded signals.

Laboratory studies of simulated leak signals have identified four possible source mechanisms and corresponding acoustic signatures [1]:

- air bubble--flow field interactions (broad-band, impulsive)
- turbulent flow noise (low-frequency, continuous)
- particulate collisions (broad-band, continuous)
- cavitation (broad-band, continuous)

Currently available passive-acoustic leak detection systems exploit only the large amplitude impulsive signal that results from the leak flow field interacting with air bubbles trapped in the backfill material [2,3]. This approach to leak detection, which owes its development to previous work in the field of acoustic emissions (AE), is attractive for several reasons: (1) the signal-to-noise ratio for the impulsive component of the leak signal is comparatively high, even for externally mounted sensors, (2) existing AE sensors and data acquisition equipment can be easily adapted to the AST problem, and (3) the algorithms used to detect a leak are relatively straightforward. Several problems have been identified concerning the data collection and signal processing techniques in current use. If large-amplitude, impulsive leak signals are to be reliably processed, it will be necessary to collect continuous time series, make changes in sensor array design, and implement more robust detection algorithms [1]. The problem with passive-acoustic leak detection systems, however, may not be one of design, but of applicability to the problem at hand. The entrainment of air into the leak flow field is the only source mechanism identified thus far that allows for the production of large amplitude acoustic impulses. It is unknown at this time whether the required backfill conditions, and thus the impulsive signal itself, persist for actual AST leaks.

The results of laboratory and field studies [1] suggest that a combination of the source mechanisms listed above and a variety of ambient noise sources will contribute to the observed AST acoustic signal. The ideal approach to data collection and signal processing would allow any type of leak signal, whether impulsive or continuous, to provide useful information regarding the location of a leak. Detection/location systems that utilize beam-forming techniques [4] have proved successful in exploiting both impulsive and continuous signals in many applications (e.g., ocean acoustics). Beam-forming involves the coherent addition of time series obtained from the individual array elements. By introducing appropriate time delays into the individual series, the focal point of the beam can be controlled. Signals emitted from a localized source (such as a leak) that remain correlated over the array aperture will be enhanced through the beam-forming process, while uncorrelated noise will be reduced. A portion of this work will address the possibility that beam-forming techniques capable of exploiting a wide range of leak signals may be applied to the AST leak detection problem.

Under the sponsorship of the American Petroleum Institute (API), several fundamental questions regarding AST passive-acoustic leak detection were addressed through a series of experiments performed on a 114-ft-diameter tank located at the Mobil Oil Refinery in Beaumont, Texas. The primary goal of this work was to investigate the detectability of both impulsive and continuous leak signals, and to characterize the background noise field. Continuous time series of acoustic signals were recorded on wide- and narrow-aperture external sensor arrays and internally suspended hydrophones. The results of the Beaumont experiments can be summarized as follows:

- Continuous and impulsive simulated leak signals can be successfully detected using internal and external sensors.
- The external background noise level is high at low frequencies (<10 kHz) in comparison to the leak signal.
- With the exception of condensation impulses, hydrophones are unable to resolve the internal background noise field.
- Wide-aperture arrays composed of several narrow-aperture sub-arrays are desirable for leak detection. Vertical elements must be included in the array to discriminate between acoustic sources located on the AST floor (such as leaks) and sources at the product surface (such as condensation).

- Detection algorithms based on classical beam-forming techniques can be applied to the AST leak detection problem such that both impulsive and continuous leak signals may be processed.

Experiment Design

Figure 1 show a diagram of the 114-ft-diameter AST used in the experiments. JP-4 was used as the product for all experiments; the maximum product head was 17 ft. Figure 2 shows examples of typical narrow-aperture (NA) and wide-aperture (WA) external arrays used to sample the acoustic leak signal and background noise field. The hydrophones used to monitor the acoustic signals within the product were deployed through access ports located at the center and edge of the tank. Acoustic sensors used in this experiment were AET-30 resonant transducers (external) and B & K-8104 hydrophones (internal). The AET-30 combines reasonable low-frequency sensitivity with a sharp resonance near 25 kHz, thus allowing adequate reception of both continuous and impulsive leak signals; the B & K-8104 is a typical hydrophone designed to resolve low sound levels (sea-state zero) for oceanographic applications. The acoustic signals were pre-amplified by Panametrics 5660-C or B & K-2635 broadband amplifiers. A Western Graphtec TDA-3500 transient recorder capable of simultaneously sampling eight channels at frequencies up to 2 MHz was used to digitize the acoustic wave forms. Data were stored and analyzed within a COMPAQ-386 portable computer. Figure 3 shows a diagram of the apparatus used to simulate the various leak signal source mechanisms. Leak aperture diameters ranged from 0.2 mm to 3 mm, producing flow rates of approximately 1 to 10 gal/h. Continuous operation of the leak simulator was accomplished by siphoning product from the backfill container over the tank edge and into a small storage vessel. By adjusting the content and saturation level of the backfill material, different source mechanisms could be enhanced or eliminated. The saturation level was controlled by injecting air directly into the backfill material prior to the initiation of flow.

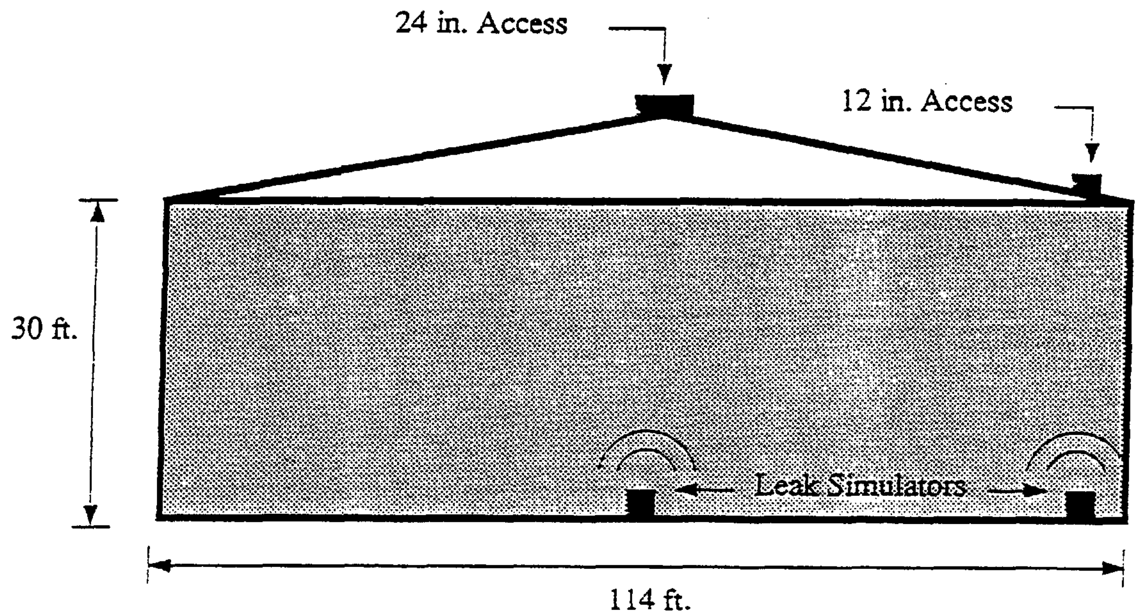

Figure 1. The 114-ft-diameter AST used in the passive-acoustic leak detection field experiment. Hydrophones and siphon-operated leak simulators were placed in the AST through 2-ft- and 1-ft-diameter access ports located near the center and edge of the tank. All tests were conducted with JP-4 as the product at levels between 10 and 17 ft.

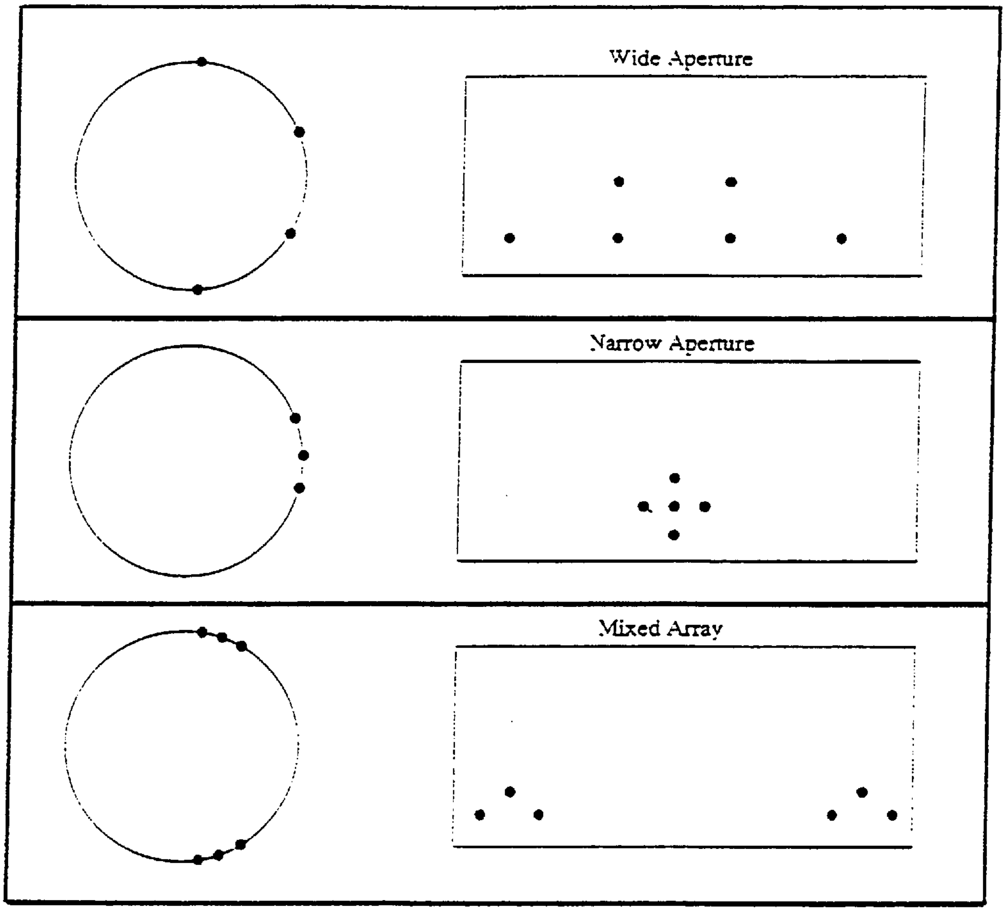

Figure 2. Typical external array geometries used in the experiment. Wide-aperture arrays provide increased spatial resolution while narrow-aperture arrays minimize time-registration errors in processing acoustic data. AET-30 acoustic transducers were used as external sensors.

Experiments were conducted over a three-week period during May 1991. A typical data set for a given array geometry, leak flow rate, and backfill condition consisted of 5 to 10 "leak-on" measurements bracketed by a pair of "leak-off" measurements. Sample rates for signal digitization ranged from 10 to 100 kHz resulting in data sets of up to 10 s in duration. Though some ambient noise sources (wind, condensation, precipitation, transportation noise) could be minimized through appropriate scheduling of data collection, other sources associated with the normal operations at a refinery were present under all experimental conditions. In general, the acoustic background noise level external to the AST was consistently high.

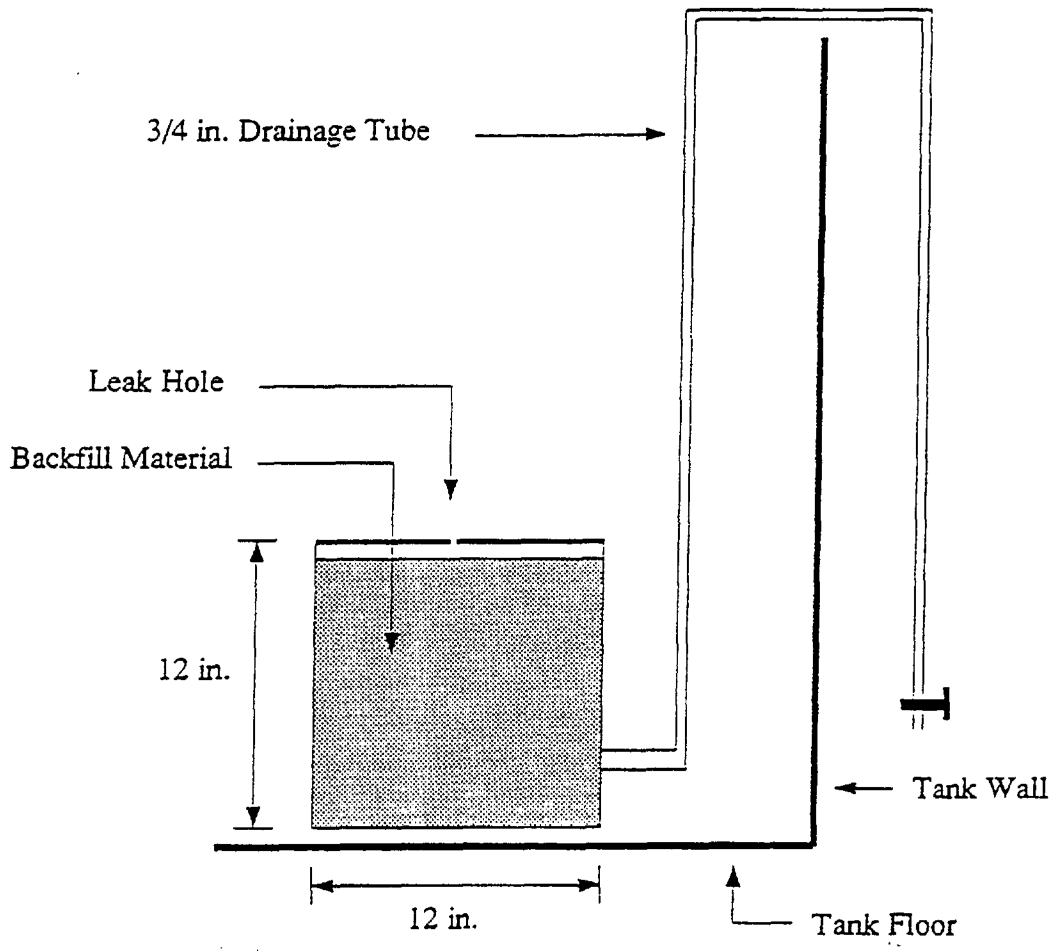

Figure 3. Leak simulator designed to siphon product through a small-diameter hole and a layer of backfill material to produce the acoustic leak signal. Backfill materials used in the experiment were product (JP-4), coarse gravel, and fine-grain sand.

Detection of Impulsive Leak Signals

The operation of a passive-acoustic AST leak detection system presently requires that large-amplitude, impulsive signals be produced by the leak. Information concerning the leak consists entirely of sets of impulse arrival times measured at spatially separated locations; time series of the acoustic signal are generally not recorded. Each set of arrival times is converted to a source location estimate through the application of a relatively simple detection algorithm. In order for such a system to perform well, three conditions must be met: (1) the impulsive signal must exist, (2) the impulsive signal must be detectable over the AST dimensions, and (3) arrival time sets must be dominated by single impulsive events as opposed to mixtures of several impulses and/or reverberation signals. Condition (3) is related to the threshold level used to trigger data collection at each sensor and the element spacing within the acoustic array [1]. The detectability of impulsive signals over typical AST dimensions was investigated during the Beaumont experiments. In order to simulate the type of impulsive leak signal that would be expected from an AST leak into a well-drained backfill, a moderate amount of air was injected into the leak simulator backfill material prior to the initiation of flow. A near-field acoustic sensor located 10 cm from the leak simulator was used to verify that the simulated impulsive leak signal was similar to the type of impulsive signals observed under laboratory conditions.

Approximately 70 data sets of 0.5 s duration each were recorded over a three-day period during which impulsive leak signals were investigated. Figure 4 shows a typical data set recorded with a four-element, wide-aperture array in the presence of a 3-gal/h leak into a sand backfill; a leak-off time series recorded on one of the array elements is shown for reference. These time series are typical examples of the type of impulsive signals recorded. The maximum distance between the leak source and the array elements is 85 ft for this data set. Based upon a visual inspection of the time series of Figure 4, the signal produced by the entrainment of air bubbles into the leak flow field should be easily detected. If the backfill beneath a real AST leak contains air, either through natural drainage mechanisms or by pressurization, the resulting large-amplitude, impulsive leak signal should be detectable using externally mounted transducers. The problem of leak detection and location is then reduced to one of choosing the optimum array geometry, correctly processing the acquired data, and minimizing the effects of ambient noise sources.

The time series shown in Figure 4 can be used to demonstrate the difficulty that AE detection algorithms have in correctly processing the information contained in impulsive leak signals. The largest amplitude impulse occurs near the 70-ms point for array elements 1 and 2, and near the 85-ms point for array elements 3 and 4. The arrival times for this impulsive event are consistent with the known leak location; thus, if these four arrival times could be measured and used as input to a detection algorithm, an accurate estimate of the leak location would result. The procedure by which AE-based leak detection systems currently process data such as that shown in Figure 4 is as follows. For each element of the sensor array, an impulse arrival time is recorded when a preset threshold signal level is exceeded. The source location estimate is then obtained by applying a location algorithm to a set of impulse arrival times. The threshold signal level is based upon the rms output of the sensor, and the rate at which arrival times are recorded is inversely proportional to the threshold setting. If the thresholds for the array elements are set too low, many sets of arrival times are collected, but a large fraction of these sets are produced by noise (both system and background) or mixtures of several impulsive events [1]. If the thresholds are set too high, the number of source location estimates is not large enough to provide the statistics necessary to view the leak as distinct from the background noise field. Figure 4 contains useful information regarding the leak location. Suppose that this information is processed, using the AE-based technique outlined above, such that an accurate location estimate can be made. A simple analysis shows that the ratio of the threshold signal level to the rms signal level for each sensor element must be set within the range $6.5 < V_t/V_{rms} < 7.5$ in order for a single, accurate location estimate to result from the processing of this particular 0.25 s of data. Threshold levels set below or above this narrow range result in either no impulsive events being recorded, or the recording of one or more impulse arrival time sets that produce inaccurate location estimates. Leak detection systems that gather and process only impulse arrival times would therefore have to discard a great deal of information concerning the leak location, even in the presence of relatively strong signals, in order to assure that the information that *is* processed results in accurate location estimates.

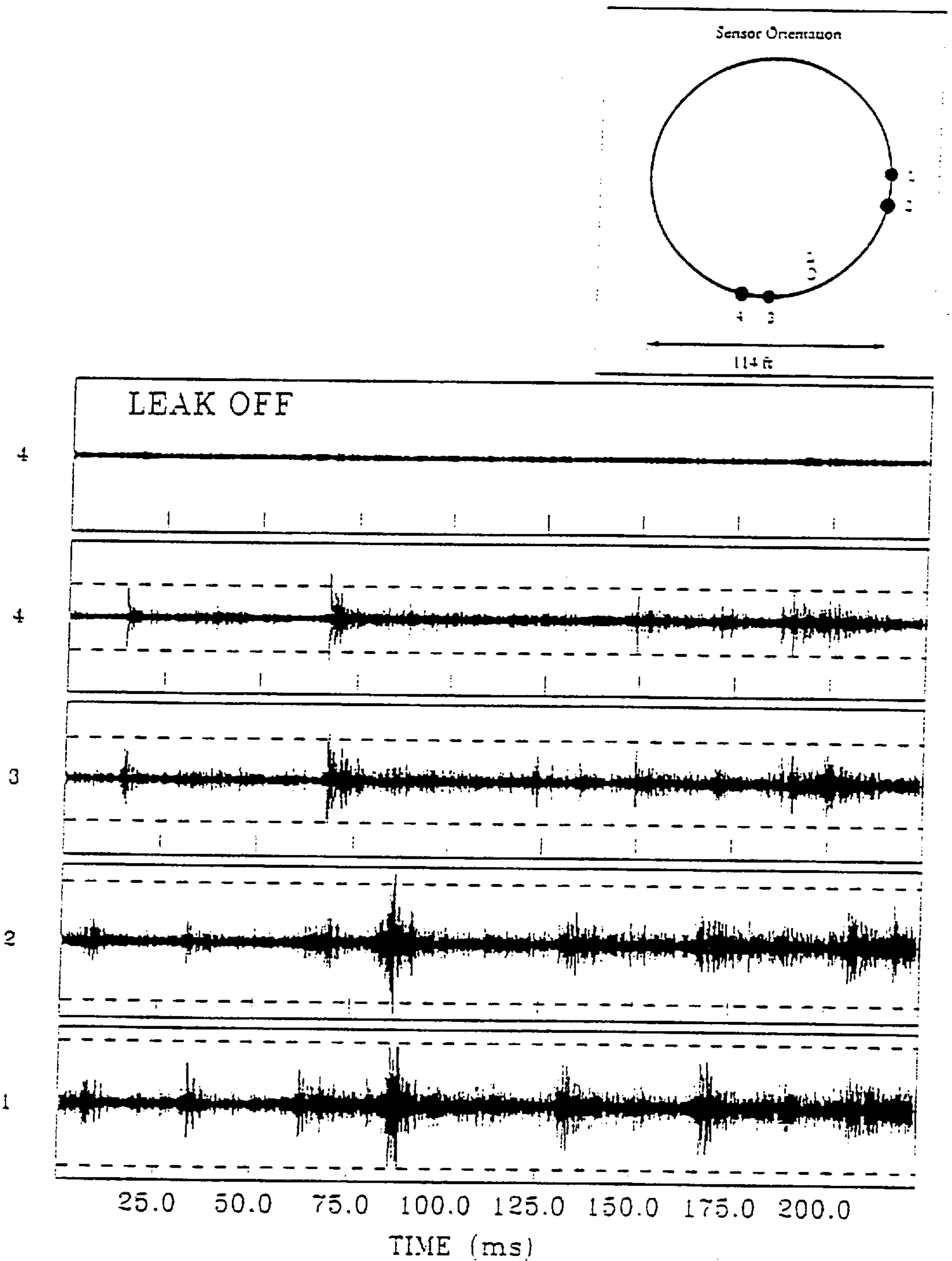

Figure 4. Time series of acoustic leak signals recorded by a four-element, wide-aperture external array. The flow rate for this experiment is 3 gal/h into an unsaturated sand backfill; the sampling rate is 50 kHz. Sensor and leak simulator positions are shown for reference. Also included is a time series recorded immediately prior to the initiation of flow under no-leak conditions. Dashed lines indicate threshold signal level at $7 \cdot V_{rms}$

Detection of Non-Impulsive Leak Signals

The large pressure gradient across a hole in the floor of an AST creates turbulence within the leak flow field. In the absence of cavitation, turbulent flow produces an acoustic signal that is continuous and primarily concentrated at lower frequencies with a high-frequency cutoff dependent upon the diameter of the leak. If the pressure fluctuations within the flow field are great enough, cavitation can be induced. The collapse of vapor pockets associated with cavitation and the entrainment of air associated with a non-saturated backfill produce impulsive leak signals in a similar manner. The sampling rates typically used in this experiment (10 to 100 kHz) are high with respect to the rate at which air bubbles are entrained into the leak flow field. The signal thus appears as a set of distinct impulses in the recorded time series. The collapse of cavitation-induced vapor pockets, which occurs at a much higher rate, produces a signal that appears to be continuous in the time series. Turbulent flow can cause collisions between backfill particulates and the tank bottom. As is the case with cavitation, the sound produced by this impulsive source mechanism is viewed as continuous in time series sampled at a rate substantially lower than the collision frequency.

Figure 5 shows a leak signal time series recorded on an external sensor located 85 ft from a 5-gal/h simulated leak. The backfill material is saturated sand and the leak diameter is 1.0 mm. A no-leak time series recorded on the same sensor immediately prior to the initiation of flow is shown for reference. Removing the air bubbles from the backfill eliminates large amplitude impulses from the leak signal. The observed difference between the signal level recorded under no-leak conditions and the signal level recorded with the leak present indicates that the non-impulsive signal is detectable in the far field of the leak. Figure 6 shows the signal-to-noise ratio obtained from the ratio of the power spectral densities of the leak signal and background noise for the time series of Figure 5. The signal-to-noise ratio is greatest in the frequency range beyond 10 kHz. A background noise power spectral density plot for the external sensors is shown in Figure 7. The signal-to-noise ratio is greatest at frequencies above 10 kHz, corresponding to a sharp reduction in the background noise level. The time series used to compute the background noise spectrum were recorded late at night under relatively calm conditions to avoid transportation-related noise and the effects of wind stress on the AST. Steam leaks from aboveground pipelines in the vicinity of the experimental site are believed to be the dominant source of background noise. The broad peak in the background noise spectrum from 1 to 10 kHz is large enough to obscure measurements of the far-field continuous leak signal at low frequencies.

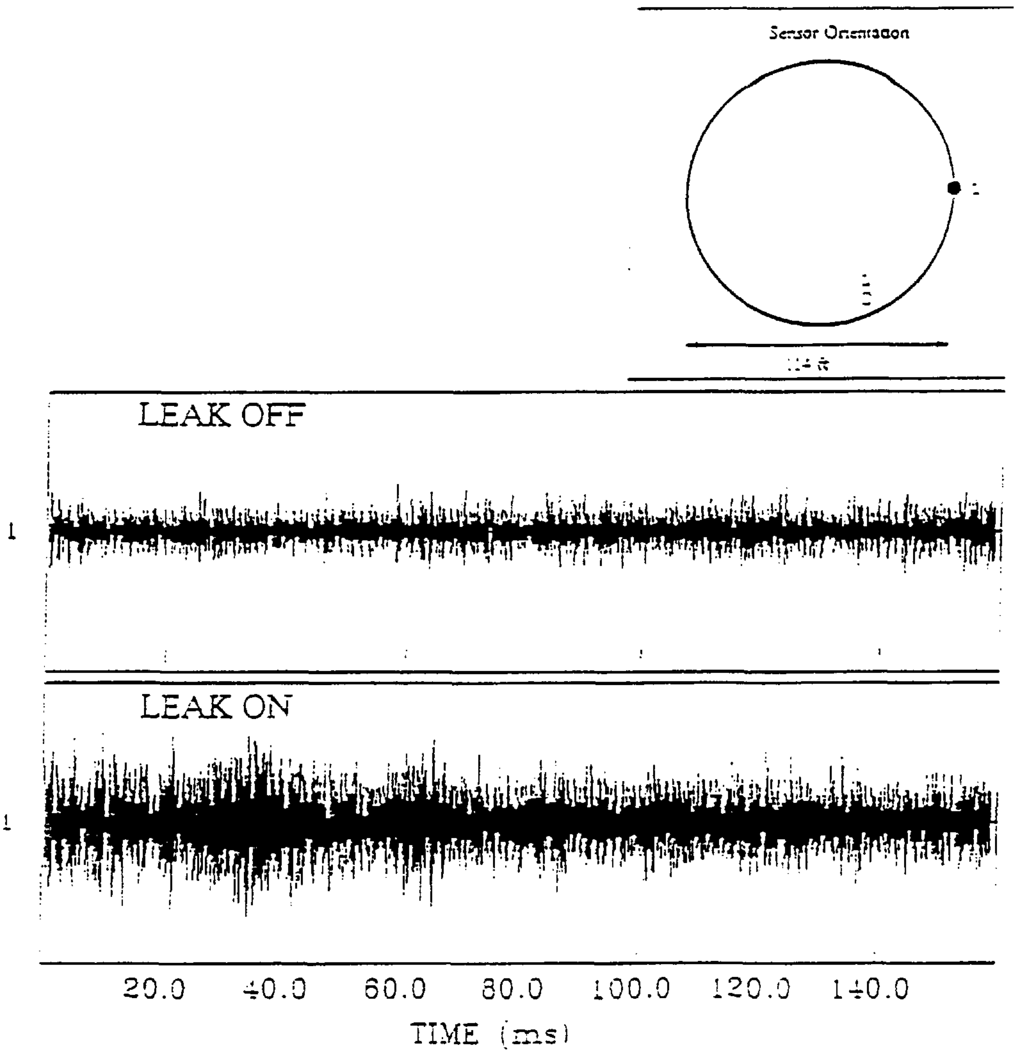

Figure 5. Time series of acoustic signals recorded under leak-on/leak-off conditions by an external sensor positioned 85 ft from the leak simulator. The flow rate for the leak-on series is 5 gal/h into a saturated sand backfill; the sampling rate is 50 kHz. Sensor and leak simulator positions are shown for reference.

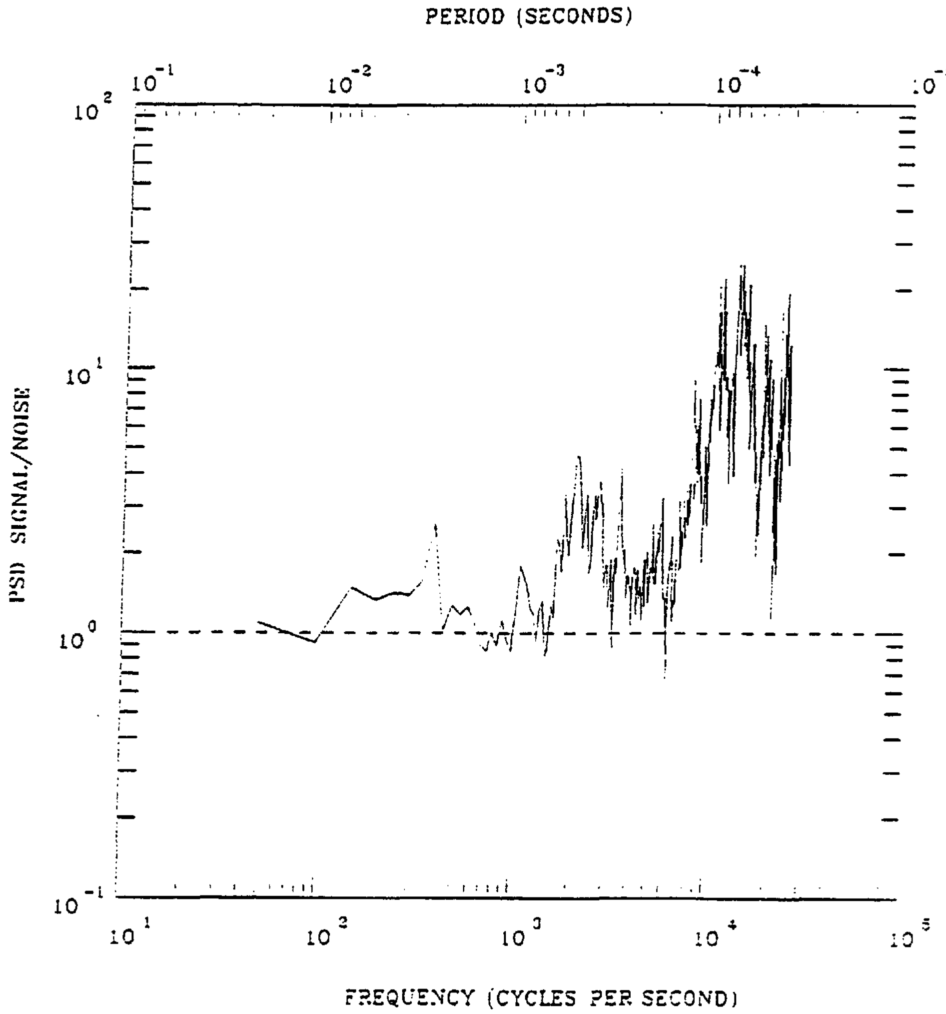

Figure 6. Ratio of power spectral densities computed using the leak-on and leak-off time series of Figure 5. Each PSD represents an average of 31 1024-point FFTs individually detrended and weighted with a cosine bell. A signal-to-noise ratio of 1 is indicated by the dashed line.

The successful detection of a source of acoustic signals using an array of transducers requires a degree of similarity between signals received at spatially separated locations. If the output of a pair of separated sensors is highly correlated and the source of the measured signal is localized, the relative arrival time of the signal at each sensor location can be extracted from the time series. These relative arrival times then serve as input to a detection algorithm. The degree to which the received signals maintain their similarity over the length of the array determines the accuracy with which the source location is estimated. A quantitative measure of this similarity is obtained by computing the complex coherence as a function of frequency between pairs of time series. Figure 8 shows the squared-coherence amplitude and phase for time series of continuous leak signals recorded in the far field of the leak with sensors separated by approximately 6 ft. At frequencies where the squared-coherence amplitude is high (e.g., exceeding the 95% confidence level), the coherence phase can be used to estimate the relative time of arrival of the signals at

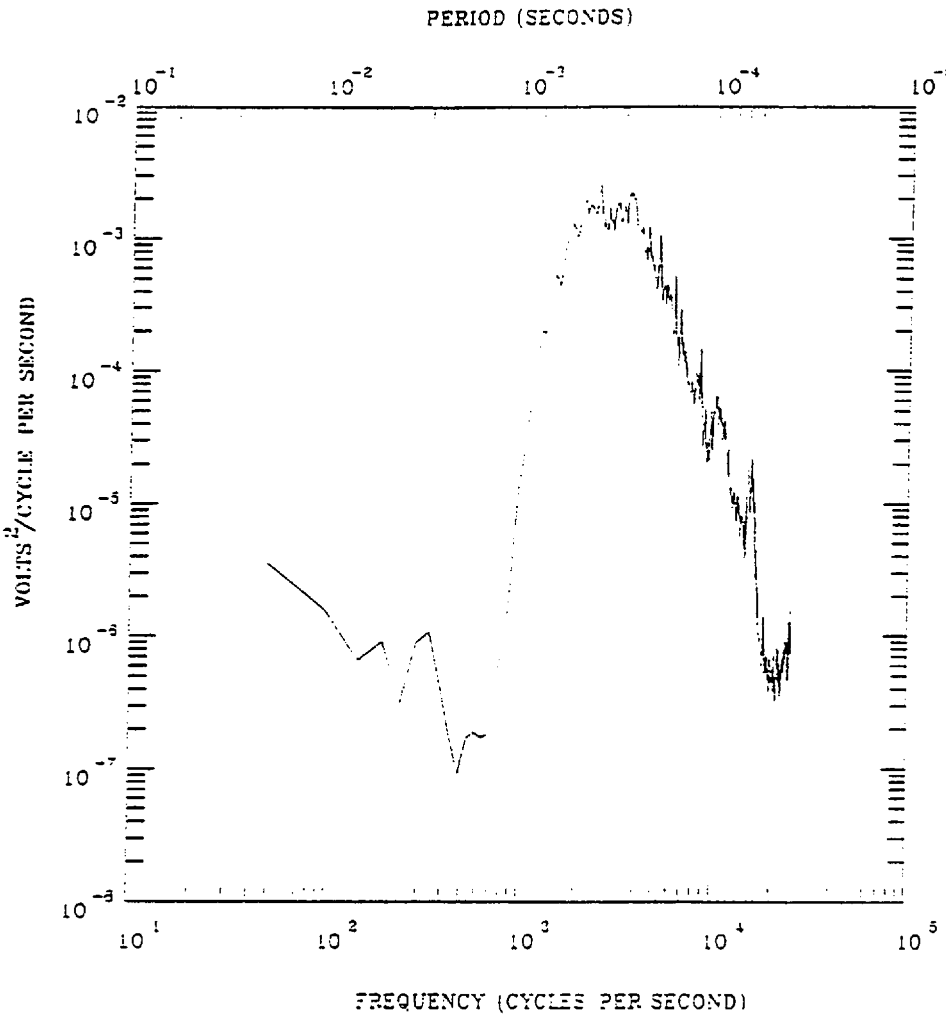

Figure 7. Power spectral density of background noise recorded by a four-element external array. The corresponding time series were recorded late at night under relatively calm ambient conditions. The PSD represents 31 1024-point FFTs averaged over the four sensors.

each sensor. In order to unambiguously measure the phase difference between a pair of sensors, and hence the relative arrival time, the sensor separation should be on the order of a half-wavelength of the received signal. For a narrow-aperture array with element spacings of 1 m and signals propagated in JP-4 (c ~ 1250 m/s), this means that the coherence amplitude should exceed the 95% confidence level within a frequency band centered at ~1 kHz. The data presented in Figure 8, in which statistically significant coherence is observed only at frequencies above 10 kHz, suggest that simply extending the presently used location algorithm to include continuous leak signals will be difficult. In environments where the ambient noise level is extremely high, such as refineries, passive-acoustic leak detection systems that utilize externally mounted sensors may require the collection of long time series, in combination with a beam-forming algorithm that enhances marginally coherent signals while suppressing uncorrelated noise, in order that the information contained within continuous leak signals can be processed toward an accurate leak location estimate.

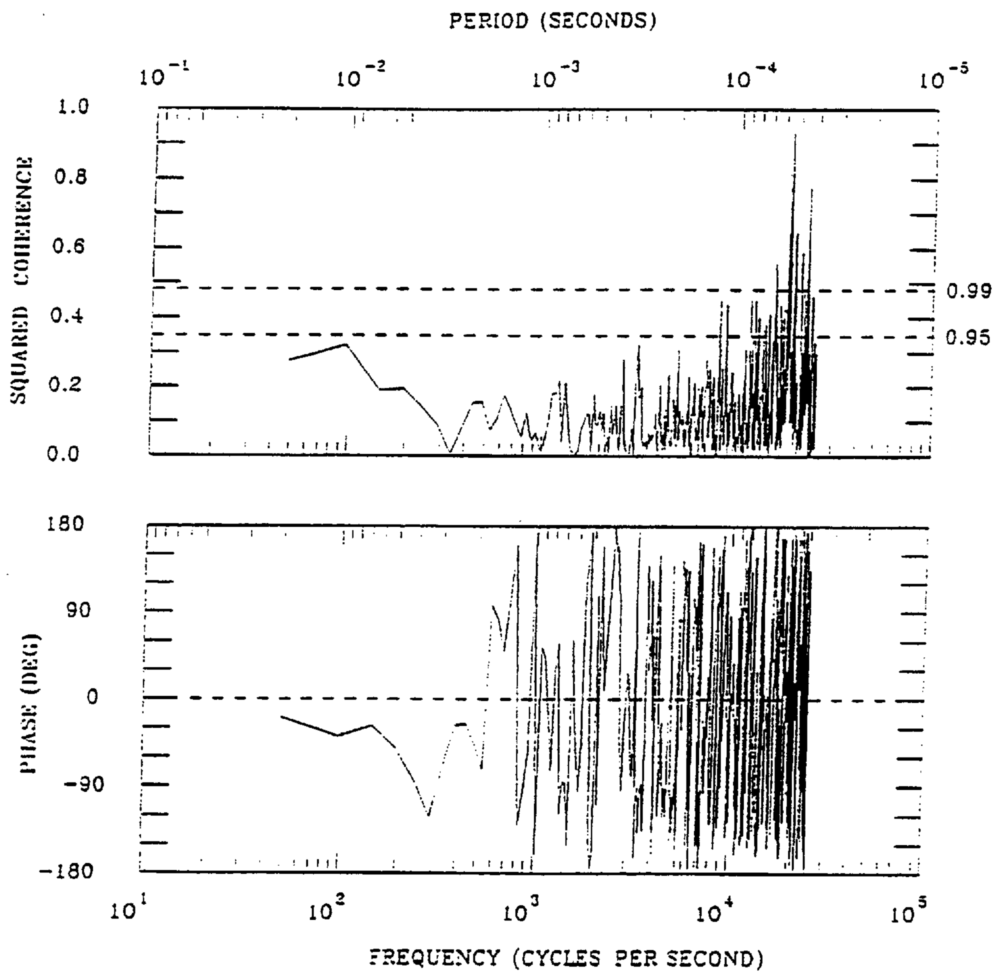

Figure 8. Complex coherence function (amplitude and phase) computed between time series of continuous leak signals recorded by external sensors. The flow rate is 5 gal/h and the backfill material is saturated sand. Sensor separation is approximately 6 ft; distance between leak simulator and sensors is 85 ft. Confidence levels are indicated by dashed lines.

Detection of Low-Frequency Leak Signals

The presence of a low-frequency component of the leak signal produced by flow into a saturated backfill can be verified by either moving the external sensor array into the near field of the leak, or by using sensors suspended in the product. Time series were recorded on a pair of hydrophones suspended at a distance of 60 ft from the leak simulator and separated from each other by approximately 2 ft. An estimate of the signal-to-noise ratio (SNR) for the low-frequency component of the leak signal, shown in Figure 9, was obtained by dividing the power spectral density computed with the leak present by a similar spectrum computed with no leak present. The leak-on and leak-off power spectra for the individual hydrophones were averaged together prior to computing the SNR; the time series used were 1.7 s in duration sampled at a frequency of 10 kHz. The backfill material used for this measurement was saturated gravel; the flow rate was 5 gal/h through a 1-mm-diameter hole. The squared-coherence amplitude and phase between the two hydrophones are shown in Figure 10. The signals remains coherent over the 2-ft sensor separation up to a frequency of approximately 600 Hz, and the 0° phase difference between the two signals is consistent with the sensor orientation. Figure 11 shows the squared-coherence amplitude and phase between time series recorded by a pair of external sensors located approximately 30 ft from a continuous leak signal source; the separation between the two sensors is 3 ft. Coherence above the 95% level of statistical significance is observed at several frequencies below 1 kHz. Though the coherence is not high over a broad enough frequency band to estimate the relative arrival time of the leak signal, the source of this simulated leak was located to within 3 m by applying a beam-forming algorithm to data recorded using a four-element, narrow-aperture array.

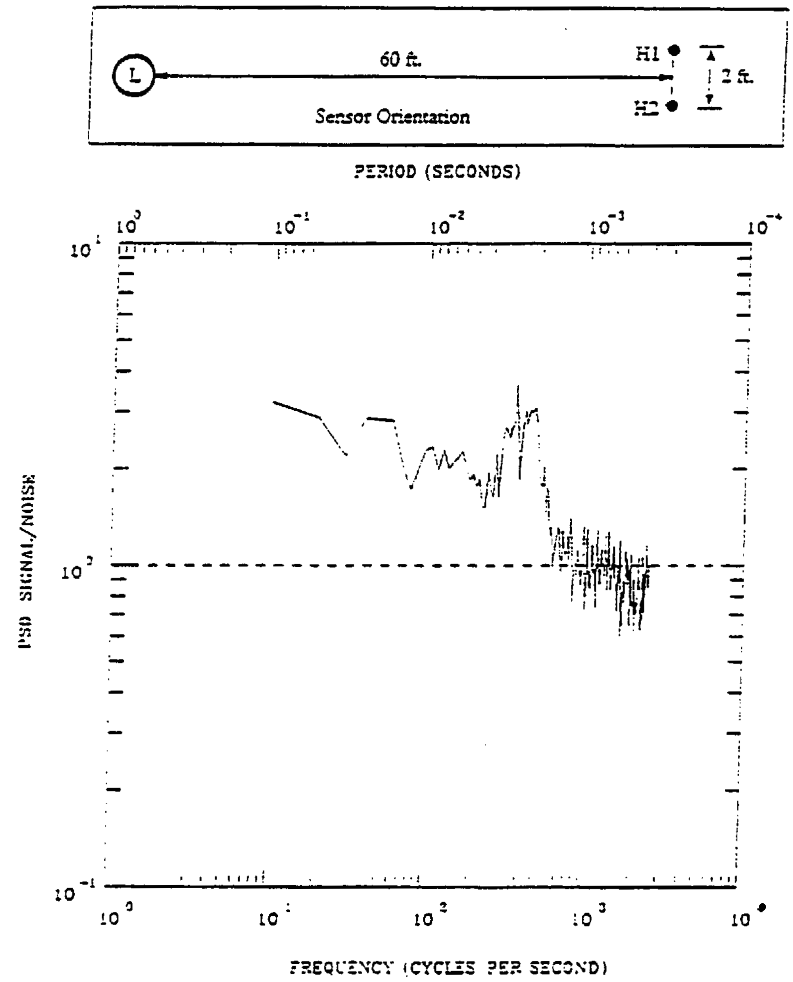

Figure 9. Ratio of power spectral densities of leak-on and leak-off time series recorded by hydrophones located in the product. The flow rate is 5 gal/h and the backfill material is saturated gravel; the sampling rate is 10 kHz. Sensor separation and leak simulator position are shown for reference.

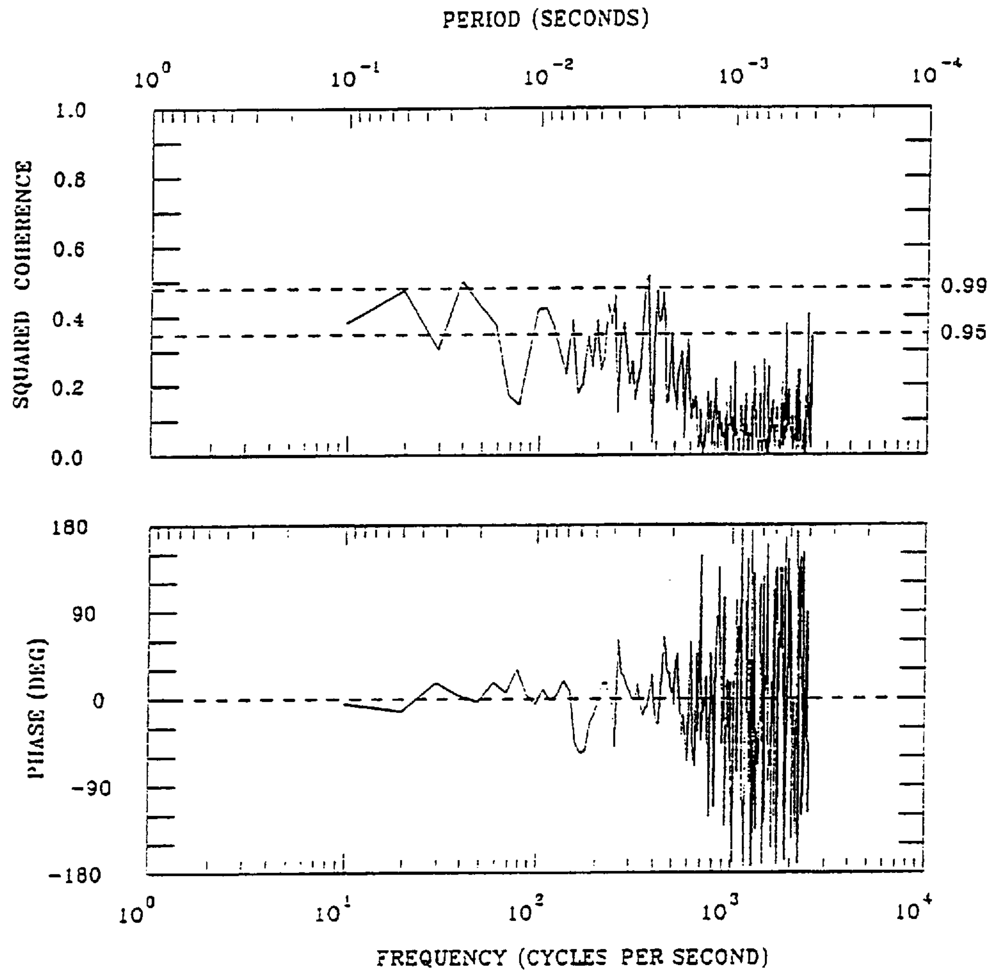

Figure 10. Coherence and phase computed between time series recorded by hydrophones. Sensor separation is 2 ft; distance from leak simulator to sensors is 60 ft. The flow rate is 5 gal/h and the backfill material is saturated gravel; the sampling rate is 10 kHz. Confidence levels are indicated by dashed lines.

When the dominant component of the acoustic leak signal is continuous, rather than impulsive, the design of a leak detection system is made more complicated both from a hardware design and a signal processing perspective. If the continuous leak signal is of sufficient strength, processing techniques such as coherence function analysis may be used to measure the relative arrival times of the leak signal at the various sensor locations, provided that continuous time series are recorded. These arrival times may then serve as input to the same detection algorithms currently used in AE-based detection systems. If the signal is weak, or equivalently, if the background noise level is high, beam-forming techniques that require the collection of long time series may be used to map out the acoustic intensity on the tank floor. Passive-acoustic systems utilizing this approach have been successfully applied to ocean acoustics, jet engine, and

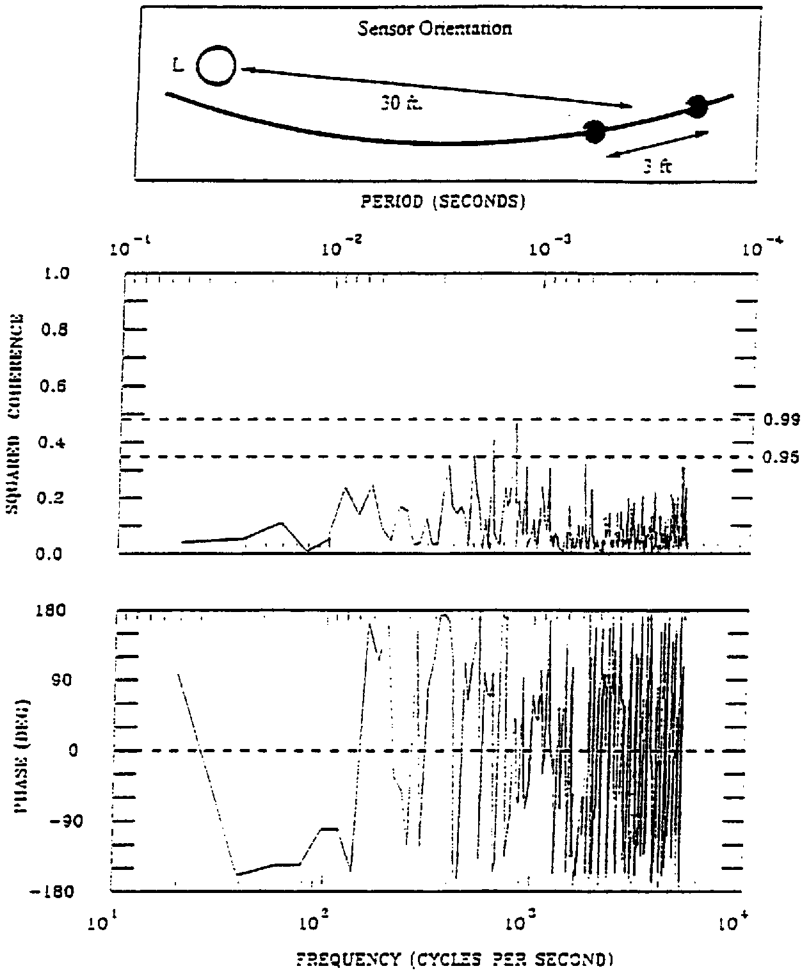

Figure 11. Coherence and phase computed between time series recorded by external sensors in near field of leak. Sensor separation is 3 ft; distance from leak simulator to sensors is 30 ft. The flow rate is 5 gal/h and the backfill material is saturated gravel; the sampling rate is 10 kHz. Sensor separation and leak simulator position are shown for reference.

helicopter-rotor noise source location problems [5-7]. The *Analysis* portion of this work will explore the possibility that these same sound-level mapping procedures may be applied to the problem of detecting AST leaks.

Analysis

Experiments using simulated leaks within a 114-ft-diameter AST have shown that continuous and impulsive acoustic leak signals produced by leaks of between 1 and 5 gal/h are detectable. The degree of control provided by the leak simulator enables simulated leaks to be detected through a difference in the leak-on/leak-off time series or power spectra. Since no such control mechanism currently exists for real AST leaks, the detection of leaks must be done by measuring the average acoustic intensity over the entire AST floor and identifying regions within which the local intensity greatly exceeds this value. The end result of this detection-through-location process, whether based upon measurements of sets of impulse arrival times or continuous time series, is an estimate of the sound level as a function of position on the AST floor. The choice of a specific leak detection algorithm is dependent upon the characteristics of the leak signal and the background noise field in which the signal is immersed. For impulsive leak signals, a detection algorithm that processes only relative arrival times of impulses may provide an adequate acoustic map of the AST floor provided that (1) the impulses are of sufficient amplitude to be detected with a threshold set well above the average signal level, (2) the mixing of impulses and/or noise outlined in [1] is avoided, and (3) no strong source of impulsive noise, such as condensation, is present. Experimental data indicate that these conditions are not likely to be satisfied for real AST leaks within full-scale tanks, even in the case of partially saturated backfills. The time series shown in Figure 4 contain several impulsive events, the arrival times of which are each consistent with the known leak location. Due to differences in the propagation paths from leak-to-sensor and the sensor/shell coupling, significant variations in impulse amplitude are observed among the array elements. Also, the frequency with which impulses are emitted from the leak is relatively high ($\sim 20\ s^{-1}$). The combination of rapid impulse emission, long transit lengths (hence reduced amplitudes), and variations in received signal for a given impulse produce a leak signal that is unlikely to be processed accurately by AE-based leak detection systems. The case against discrete arrival time algorithms is further strengthened by the observation that impulsive leak signals require an unsaturated backfill, and thus may not persist for a large class of real AST leaks.

The detection strategy currently in use is designed to detect strong signals in a weak noise field. Though very little data have been published concerning the characteristics of real AST leak signals, it seems likely that the detection problem should be approached as one of detecting relatively weak acoustic signals in a strong noise field. Several source mechanisms have been identified that produce persistent, measurable leak signals. The information provided by continuous time series of persistent leak signals combined with signal processing algorithms appropriate for use in low signal/noise ratio environments may serve as a better technique for detecting many AST leaks.

Beam-Forming Algorithm

The proposed approach is based upon focused beam-forming techniques developed for radar and oceanic detection problems [4]. Figure 12 presents a diagram of a focused beam-forming detection algorithm. Signals received by spatially separated sensors are amplified, digitized, filtered, time-delayed, and coherently added to form a summation series referred to as a beam. By adjusting the relative time delays among the array elements, this beam can be steered over the entire AST floor and processed to yield the received acoustic energy as a function of position.

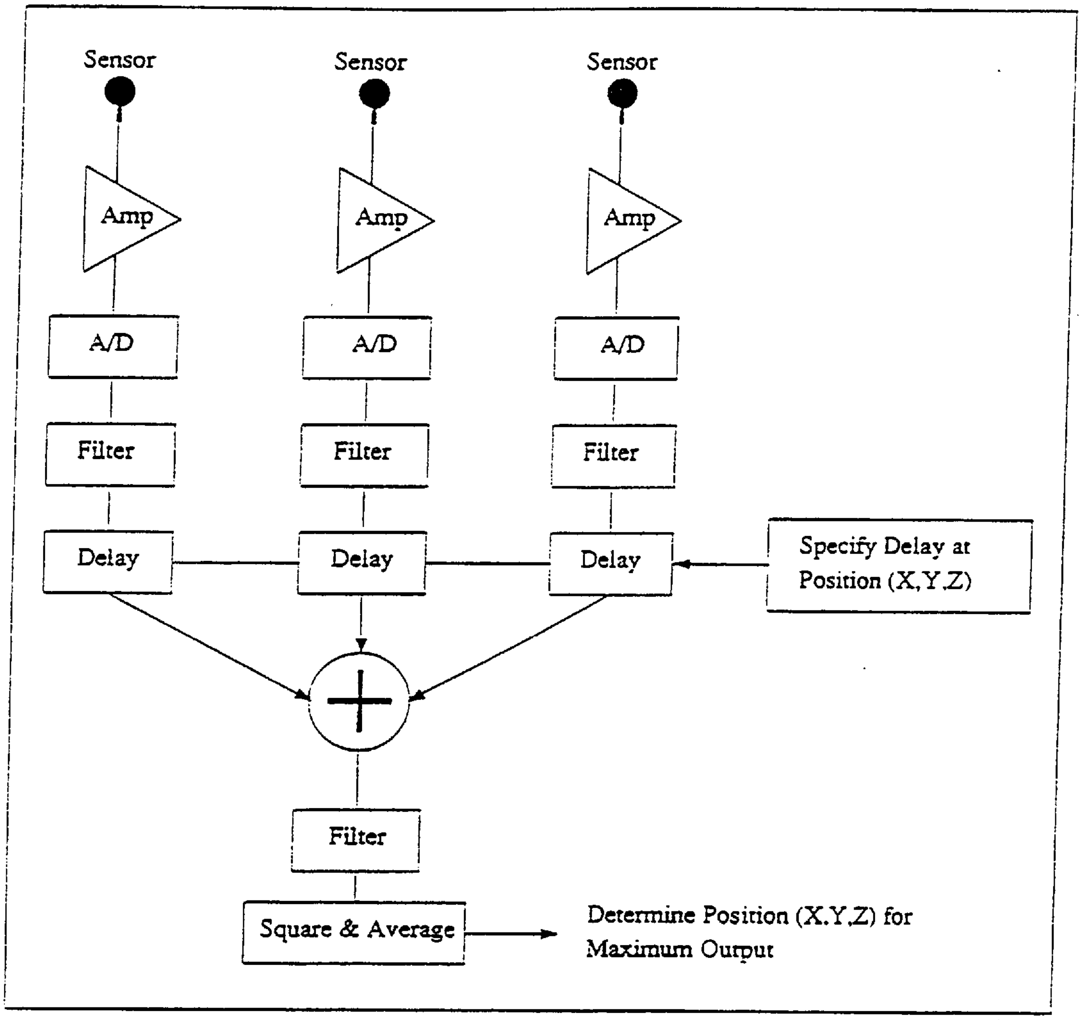

Figure 12. Schematic diagram of a detection system that incorporates beam-forming techniques. Adjusting the delays for the individual time series provides a means of focusing the output beam onto a desired spatial location.

The principle of coherent addition, and its importance to the successful application of the beamforming algorithm, can be illustrated by introducing a weak, coherent signal into time series composed entirely of incoherent white noise. Such a data set can be obtained either by artificially introducing a sinusoidal signal into previously digitized time series of ambient noise, or by physically placing a weak acoustic source into the AST and collecting experimental data; the former method has been employed for this analysis. Figure 13a shows a time series for a single array element in which only ambient noise is present. Figure 13b shows the same time series in which a 3 kHz sinusoidal signal whose amplitude is 15% of the rms signal level has been added to the ambient noise. The presence of this additional signal is difficult to detect by visual inspection of the individual time series. Figure 13c shows the output time series of an eight-element sensor array that has been processed using a beamforming algorithm. In this example, the beam has been steered to obtain maximum output power through phase-alignment of the sinusoidal component of each individual time series. While the amplitude of both the pure sinusoidal signal and the noise are both enhanced through the beam-forming process, the desired signal is now clearly detectable in the time series.

The enhancement of coherent signals may be viewed in the frequency domain by computing the ratio of the total output power of the sensor array to the output power of an individual sensor element. Figure 14 shows the amount by which the coherent, 3-kHz signal of Figure 13c is enhanced relative to the noise for beamforming arrays containing four and eight sensor elements. If the number of elements in the sensor array is denoted by N, the power received by the array via the coherent, phase-aligned signals is enhanced by a factor of N^2 while the power received due to uncorrelated noise is increased by a factor of N. The gain in output power for uncorrelated noise is independent of the time-delays introduced into the individual time series. For coherent signals, however, the gain in output power is a function of the direction in which the beam is steered and attains the maximum value of N^2 when the coherent signals within each individual time series are aligned in phase. The degree to which the enhancement of coherent signals is reduced as the beam is steered away from the localized source is a function of the number of array elements and the array geometry. This difference in the output response of the sensor array to incoherent noise and coherent signals allows the sound intensity to be measured as a function of position on the AST floor.

The primary benefits of this approach are: (1) coherent signals buried in a substantial noise field can be extracted from the time series by focusing the beam on the correct source location; (2) increasing the number of array elements further enhances signals emitted from a localized source (such as leak signals) in relation to uncorrelated noise; (3) the focused beam-forming detection algorithm works equally well for strong, impulsive signals in a weak background noise field; and (4) the array geometry (number and positions of elements) may be optimized for the AST leak detection problem.

Beam-Forming Analysis Results

As a test of the proposed beam-forming algorithm, impulsive and continuous leak signals were processed to yield sound-level maps of the AST floor. Figure 15 shows time series of impulsive leak signals recorded by a four-element, wide-aperture external array in which the maximum sensor separation is approximately 85 ft. This is an example of the type of signal that could be processed reasonably well by current AE-based leak detection systems provided that the rate of impulse emission was not too high and the threshold signal levels were carefully chosen. The backfill material for this experiment was partially saturated gravel and the leak flow rate was approximately 5 gal/h; the sample rate used to collect the data was 50 kHz. The data were processed as follows: (1) a high-pass filter was applied to each time series to minimize the effects of external ambient noise at frequencies below 10 kHz; (2) the AST floor was divided into 2600 regions, and the time delays necessary to focus the acoustic beam onto each of these areas were computed; (3) at a particular focal point on the AST floor, the individual time series were delayed and then coherently added to form a summation series; (4) a segment of the summation series 16384 points in length was then squared and averaged; and (5) the squared average value of the summation signal was taken to represent the sound level at a particular point of focus. Figure 16 shows a contour map of sound level over a 400-m^2 area that includes the AST floor. The speed of sound used in the beam-forming algorithm was 1250 m/s. This value was obtained by dividing the known sensor separation by the measured relative arrival time for several large-amplitude impulses. The sound level has been normalized such that the maximum value is 1.0. The computed and actual leak locations differ by approximately 1 m. This sparse array, consisting of only four elements, produces a signal gain of approximately 5 dB, i.e., the energy received from points near the leak source is about three times as great as the received energy averaged over all tank floor positions. The observed signal gain is slightly less than the theoretical gain of 6 dB based upon the presence of coherent signals received against a background of incoherent noise.

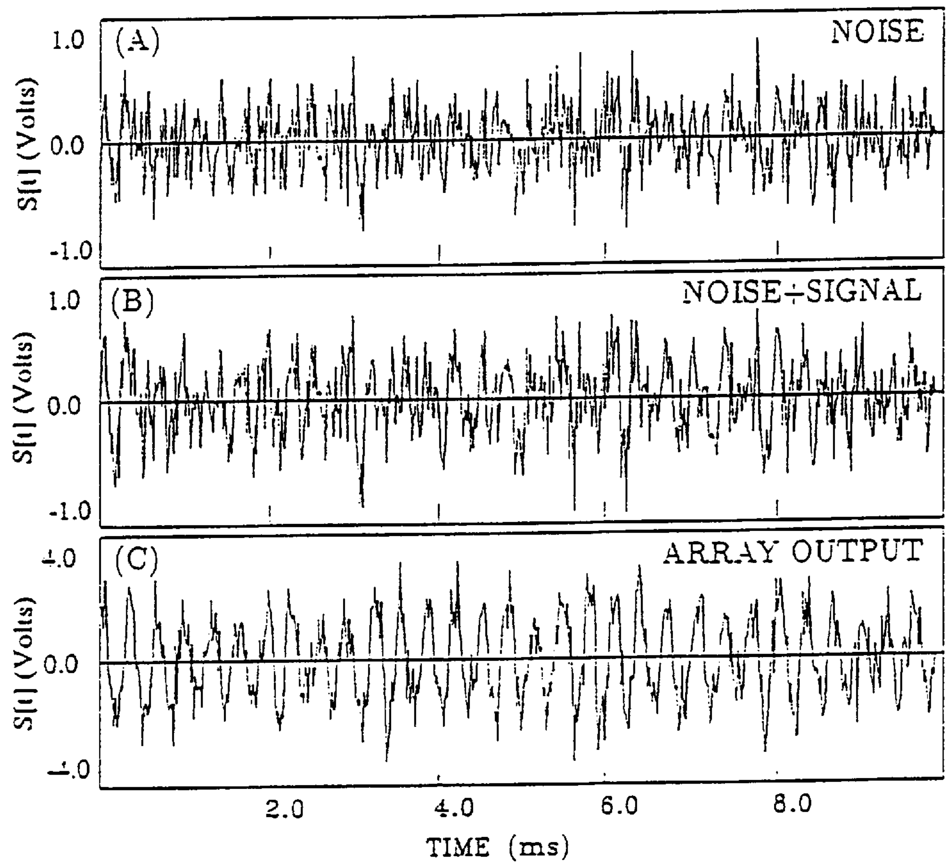

Figure 13. (a) Time series of ambient noise. (b) Time series of ambient noise plus 3 kHz sinusoidal signal of amplitude 0.3 • V_{rms}. (c) Output of beam-forming array based upon eight input signals similar to (b).

Figure 17 shows time series of leak signals recorded on a narrow-aperture array with four elements. With no leak-off time series for comparison, a simple visual inspection of the time series in Figure 17 would not reveal the presence of a leak. The backfill material used in this experiment was saturated sand and the leak flow rate was approximately 5 gal/h. The data were collected at a sample rate of 10 kHz in order to concentrate on low-frequency signals. Leak signals resulting from flow into saturated backfills, such as those shown in Figure 17, produce many false locations when processed by AE-based systems. Continuous leak signals are viewed as an additional noise source by such systems, and, consequently, their presence will act to degrade the system performance by raising the effective noise floor. A map of the sound level on the AST floor obtained through application of the beam-forming algorithm is shown in Figure 18. The data were band-pass filtered between 300 and 1000 Hz prior to formation of the

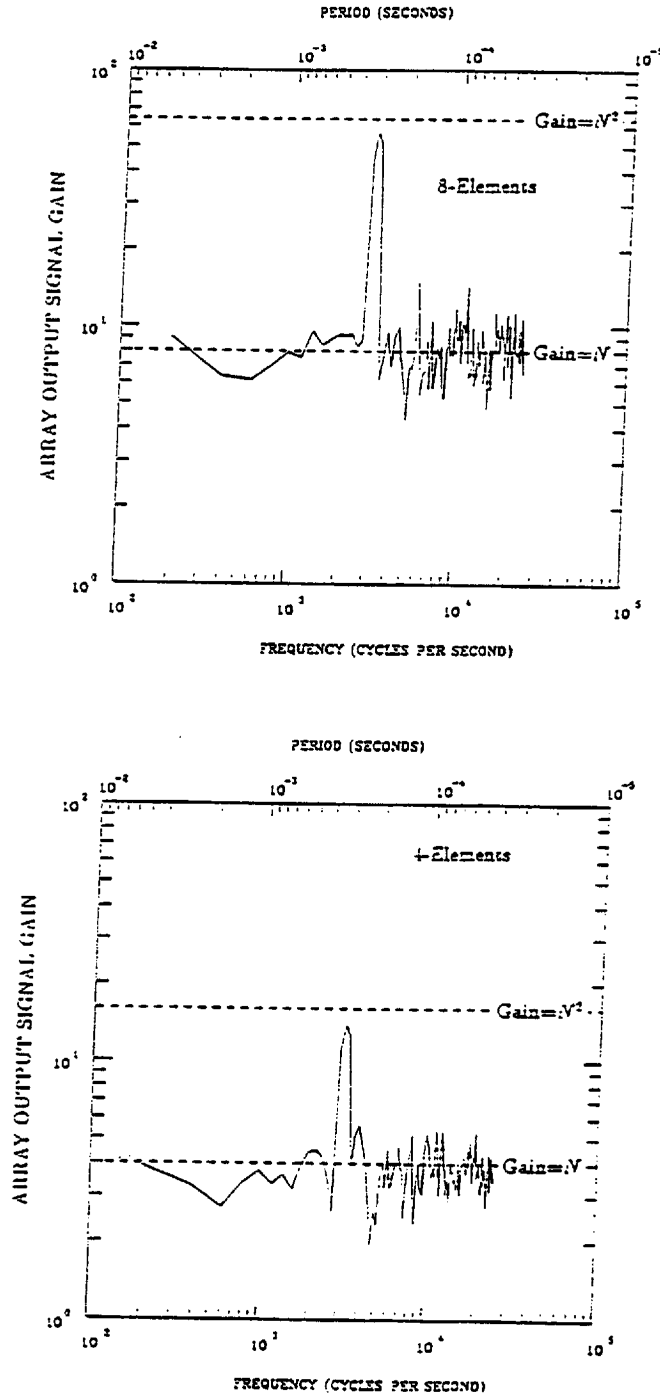

Figure 14. An array output gain defined as ratio of PSD of beam series to average PSD of individual array element series. Based upon data of Figure 13, N is the number of elements in the beam-forming sensor array.

beam. The point at which the received acoustic energy is a maximum lies approximately 3 m from the actual leak source. The signal gain is approximately 2.5 dB, approximately half of the theoretical upper limit.

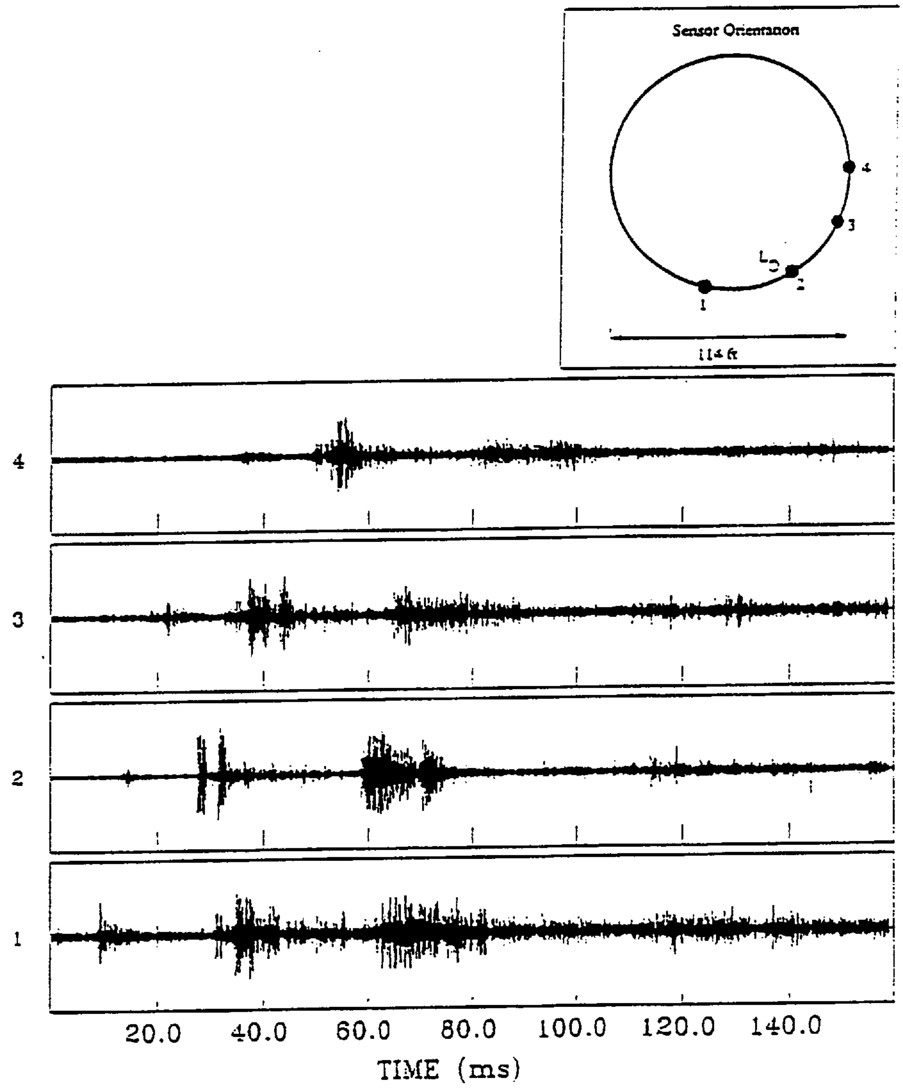

Figure 15. Time series of impulsive leak signals recorded by a four-element, wide-aperture external array. Sensor and leak simulator positions are shown for reference; the sampling rate is 50 kHz.

The errors in predicted source location for the sound-level maps shown in Figures 16 and 18 are related to differences in the amplitudes of signals received at spatially separated locations and to inaccuracies in the measurement of the array element positions. While variations in the amplitude between individual sensor elements can seriously degrade the performance of an AE-based system through time registration problems, the effect of these variations on the

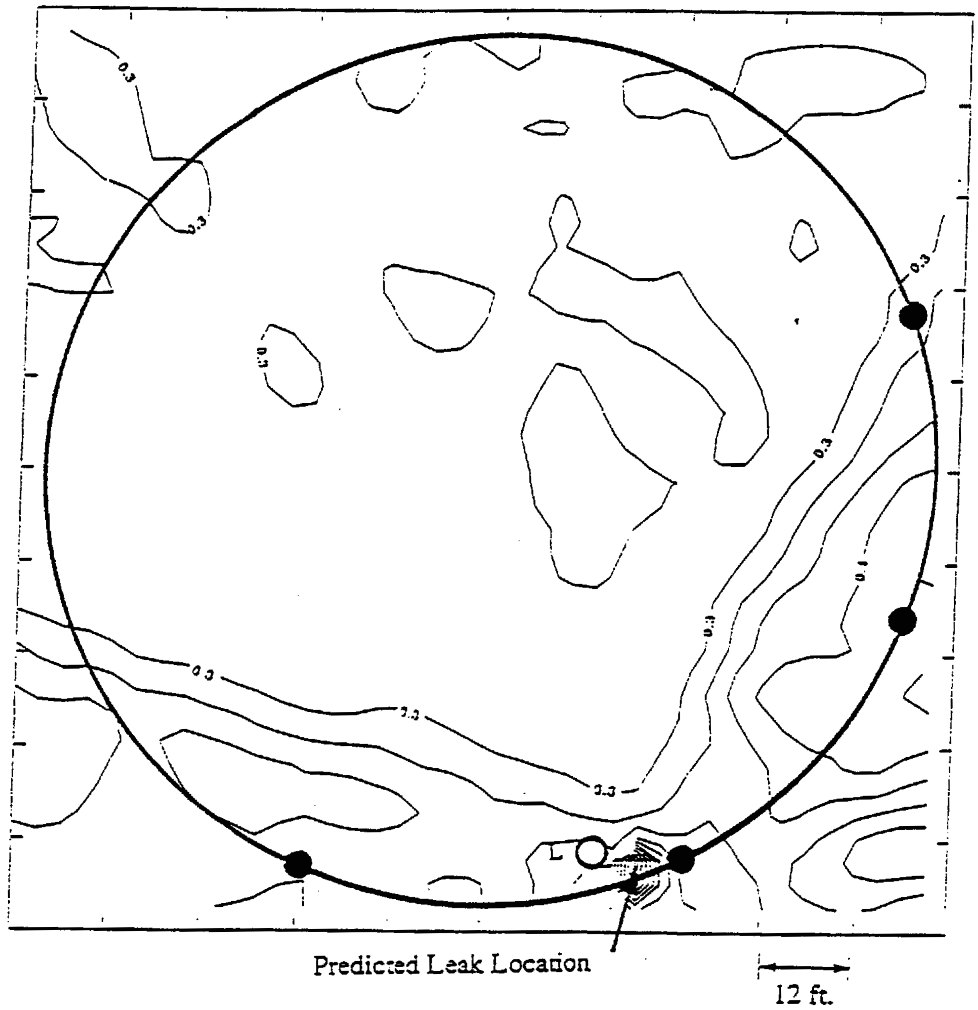

Figure 16. Results of the beam-forming detection algorithm applied to the data of Figure 15. Contours represent the normalized, average sound level as a function of position on the AST floor. Sensor and leak simulator positions are indicated. The difference between the predicted leak location (arrow) and the actual leak location is approximately 1 m.

beam-forming system is less severe. At time scales on the order of a few milliseconds or less, the time series of Figures 15 become dissimilar due to differences in sensor/tank-shell coupling, individual sensor response, and variations in the media through which the signals propagate. Averaging the output signal over the entire duration of the series, which is done as part of the beam-forming detection algorithm, minimizes the effects of time registration problems that occur over small time scales. The errors in predicted leak location introduced through inaccuracies in the measurement of sensor positions and sound velocity are systematic. Narrow-aperture arrays, while less sensitive to time registration problems, are more sensitive to these types of systematic errors due to the fact that the uncertainty in sensor position represents a relatively larger fraction of the aperture length.

The performance of a beam-forming algorithm is largely determined by four factors: (1) the SNR of the individual sensors, (2) the length of the time series upon which the detection algorithm acts, (3) the number of array elements, and (4) the relative positions of the elements within the array. The degree of control over the individual sensor SNR is strongly influenced by the particular setting in which the AST operates. In environments where the ambient noise level is relatively high and constant, such as refineries, careful attention must be paid to the remaining performance factors. If the noise competing with the leak signal is uncorrelated, significant improvements in system performance can be attained by increasing the number of array elements and the time series length. For a given individual sensor SNR, the system gain is increased by a factor of $\sqrt{2}$ by doubling the number of array elements. The standard deviation of location estimates is reduced by a factor of $\sqrt{2}$ either by doubling the number of array elements or by doubling the length of the time series that serve as input to the location algorithm.

The problem of optimizing the array geometry for the estimation of a source location in two dimensions has been addressed in [4]. Figure 19a shows the optimum array geometry for location in two dimensions in which a wide-aperture array composed of N elements is arranged in three equally spaced subarrays of N/3 elements each. An array of this type mounted horizontally on an AST would be unable to discriminate between leak signals located on the AST floor and noise sources, such as condensation, that are located above the floor. The ability to resolve vertically separated sources is gained by constructing an array similar to that shown in Figure 19b in which the N/3-element subarrays have both vertical and horizontal separation.

Conclusions and Recommendations

The analysis of data obtained during the 114-ft-diameter AST field test produced several important results. Impulsive leak signals resulting from the interaction of air bubbles with the leak flow field were found to be detectable, even against the relatively high ambient noise levels found at the Mobil-Beaumont refinery. An analysis similar to that presented in [1] concerning the application of AE-based data acquisition and signal processing techniques to acoustic leak signals has shown that modifications of the present acoustic leak detection systems must be made in order to correctly process impulsive signals. AE-based detection systems perform well only when a large fraction of the processed arrival time sets are correlated with single, impulsive events. This requirement is satisfied for high-SNR impulsive signals that are emitted infrequently and whose similarity is maintained over the dimensions of the sensor array. None of these three requirements was observed to be satisfied for simulated impulsive leak signals. The problem of improper time registration of impulsive signals must be addressed through improvements in both data collection and processing. These are discussed in [1].

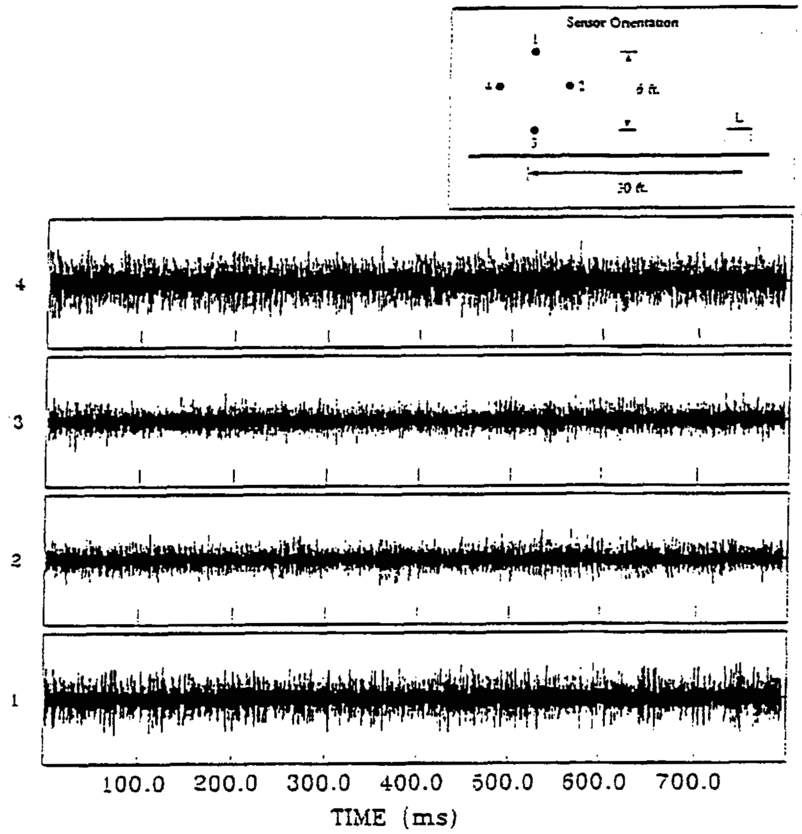

Figure 17. Time series of continuous leak signals recorded by a four-element, narrow-aperture external array. Sensor and leak simulator positions are shown for reference; the sampling rate is 10 kHz.

Continuous components of the leak signal resulting from cavitation, turbulent flow, and particulate collisions were also detectable, though the SNR for these signals was comparatively low at frequencies below 10 kHz when externally mounted sensors were employed. Because continuous signals are viewed as noise with respect to impulsive signals, the presence of continuous leak signals will act to degrade the performance of AE-based acoustic leak detection systems. While there is some question as to the persistence of impulsive leak signals due to the requirement that air be present in the backfill material, the generating mechanisms that produce continuous leak signals require only that the leak flow field be turbulent and that the backfill contain small-diameter particulates. These less restrictive criteria for producing a signal suggest that the continuous component of the leak signal may persist for a large class of AST leaks. The possibility that continuous leak signals may be exploited for the purpose of leak detection depends upon the development of a detection algorithm capable of processing continuous data and additional knowledge of the signal strength for real AST leaks.

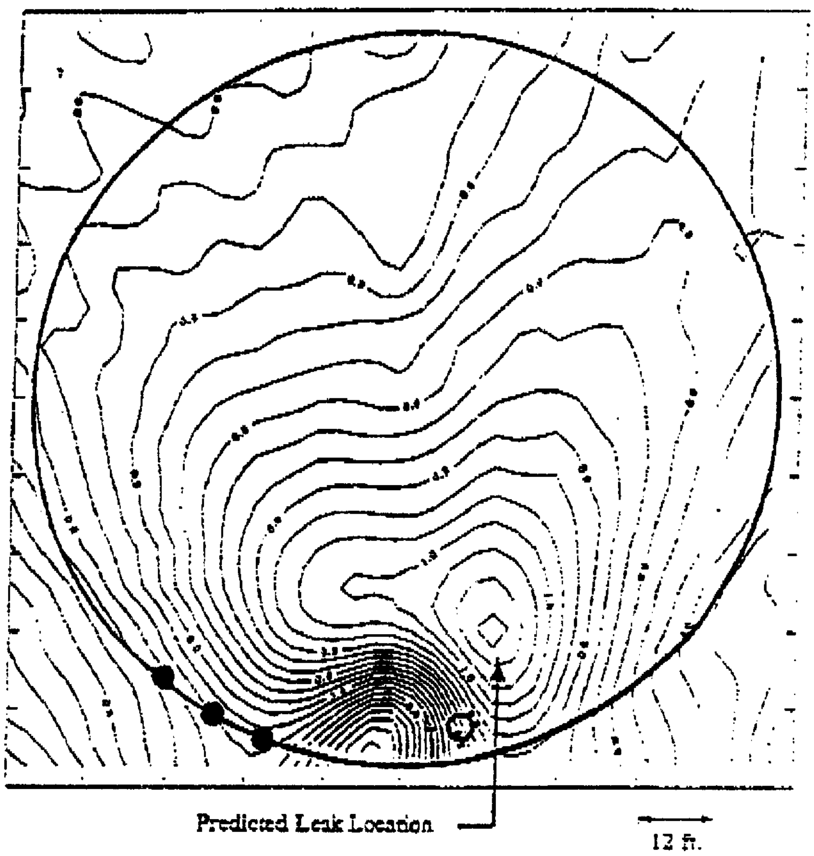

Figure 18. Results of the beam-forming detection algorithm applied to the data of Figure 17. Contours represent the normalized, average sound level as a function of position on the AST floor. Sensor and leak simulator positions are indicated. The difference between the predicted leak location (arrow) and the actual leak location is approximately 3 m.

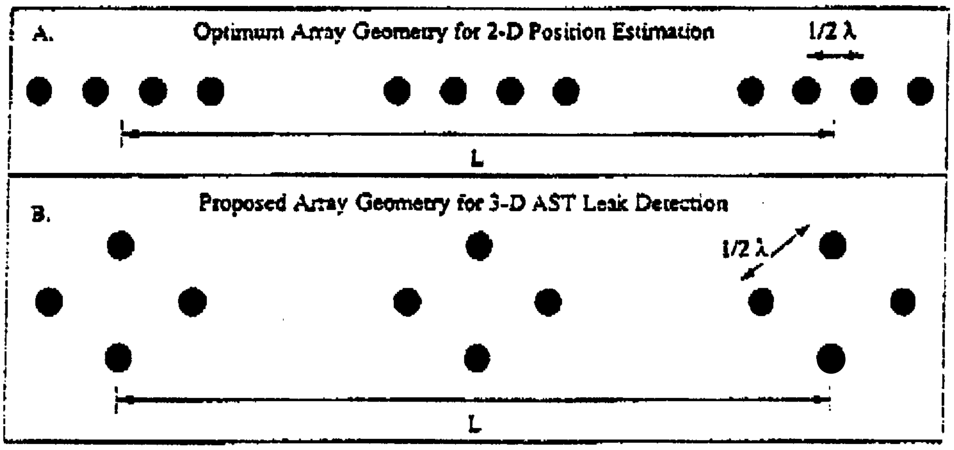

Figure 19. (a) Optimum array geometry for the location of a source in two dimensions (from [4]); (b) Proposed wide-aperture array composed of narrow-aperture subarrays for use in AST leak detection.

A beam-forming detection algorithm appropriate for use with both impulsive and continuous leak signals was developed and applied to data obtained during the Mobil-Beaumont field test. The principle behind the algorithm is one of detecting weak signals in a relatively strong noise field. Continuous time series recorded from each element of the sensor array are coherently added in order to enhance correlated signals emitted from localized sources while minimizing the contribution of uncorrelated noise. By introducing appropriate time delays into the individual time series prior to summation, the resulting beam can be steered over the entire AST floor in order to map out the sound level as a function of position. Regions of the AST floor at which the strength of the summation signal exceeds the measured, average level are interpreted as likely leak locations. The beam-forming algorithm was applied to data sets dominated by impulsive leak signals and to data obtained under saturated backfill conditions in which only the continuous components of the leak signal were present. Both applications of the detection algorithm produced source location estimates consistent with the known leak location. Significant improvements in the performance of a beam-forming detection system can be attained by increasing the number of array elements, collecting long time series, and optimizing the sensor array geometry.

The results of this experimental program are very encouraging; they suggest that passive-acoustic leak detection can be used to detect small leaks in ASTs. The experiments have shown that a detectable signal does exist, but that the current approach to data acquisition and signal processing needs to be improved for the technology to achieve its full potential. The beam-forming algorithm developed to detect a broad range of acoustic leak signals may provide a means of detection that is largely independent of the particular source mechanisms associated with a given AST leak. The beam-forming detection algorithm and data acquisition system should be refined by means of experimental data obtained from a sensor array that contains a large number of optimally spaced sensors. In addition, the uncertainty in the character of the signals produced by real AST leaks must be investigated through further experiments.

Acknowledgements. The authors wish to gratefully acknowledge the cooperation of Mobil Oil Company, and in particular John Collins of the Beaumont Refinery, for providing AST-599 and the operational support necessary for the successful completion of the experimental portion of this work. For their considerable patience and invaluable technical assistance in overcoming the many difficulties associated with the full-scale AST field test, we wish to thank Jim Starr and Richard Wise of Vista Research, Inc. We also wish to thank Det Norske Veritas, Inc., Hartford Steam Boiler Inspection Technologies, and CTI, Inc., for providing the acoustic transducers and amplifiers used in the experiment. This work was funded by a contract with the American Petroleum Institute. The authors would also like to acknowledge the encouragement and technical review provided by the API Task Force monitoring this work.

References

1. E. G. Eckert and J. W. Maresca, Jr., "Detection of Leaks in the Floor of Above-ground Storage Tanks by Means of a Passive Acoustic Sensing System," *Air and Waste Management Association*, Paper 91.15.5 (June 1991).

2. C. M. Nickolaus, "Acoustic Emission Monitoring of Aboveground Storage Tanks," *Materials Evaluation* (March 1988), pp. 508-512.

3. R. K. Miller, "Tank Bottom Leak Detection in Above Ground Storage Tanks Using Acoustic Emission," in *Proceedings of the Conference on Above Ground Storage Tanks*, Center for Energy and Environmental Management (8-9 November 1989).

4. W. S. Burdic, "Underwater Acoustic System Analysis" (New Jersey: Prentice-Hall, Inc., 1984).

5. O. E. Flynn and R. Kinns, "Multiplicative Signal Processing for Sound Source Location on Jet Engines," *Journal of Sound and Vibration*, 46 (1976) pp. 137-150.

6. T. F. Brooks, M. A. Marcolini and D. S. Pope, "A Directional Array Approach for the Measurement of Rotor Noise Source Distributions With Controlled Spatial Resolution," *Journal of Sound and Vibration*, 112 (1987), pp. 192-197.

7. G. C. Carter, "Coherence and Time Delay Estimation," in *Proceedings of the IEEE*, 75:2 (February 1987).

Order No. 849-30700

American Petroleum Institute
1220 L Street, Northwest
Washington, D.C. 20005